


## RESEARCH ARTICLE OPEN ACCESS

# Phytochemistry, Antibacterial and Antioxidant Activities of *Grewia lasiocarpa* E. Mey. Ex Harv. Fungal Endophytes: A Computational and Experimental Validation Study

Nneka Augustina Akwu<sup>1,2</sup> | Yougasphree Naidoo<sup>1</sup> | Moganavelli Singh<sup>1</sup> | Johnson Lin<sup>1</sup> | Jamiu Olaseni Aribisala<sup>3</sup> | Saheed Sabiu<sup>3</sup> | Makhotsa Lekhoo<sup>4</sup> | Adeyemi Oladapo Aremu<sup>1,2</sup> 

<sup>1</sup>School of Life Sciences, College of Agriculture, Engineering and Science, University of KwaZulu-Natal, Durban, South Africa | <sup>2</sup>Indigenous Knowledge Systems Centre, Faculty of Natural and Agricultural Sciences, North-West University, Mmabatho, South Africa | <sup>3</sup>Department of Biotechnology and Food Science, Faculty of Applied Sciences, Durban University of Technology, Durban, South Africa | <sup>4</sup>DSI/NWU Preclinical Drug Development Platform, Faculty of Health Sciences, North-West University, Potchefstroom, South Africa

**Correspondence:** Nneka Augustina Akwu ([Nneka.akwu@yahoo.com](mailto:Nneka.akwu@yahoo.com)) | Adeyemi Oladapo Aremu ([oladapo.aremu@nwu.ac.za](mailto:oladapo.aremu@nwu.ac.za))

**Received:** 6 November 2024 | **Revised:** 18 December 2024 | **Accepted:** 20 December 2024

**Funding:** Financial support was provided by the Organization for Women in Science for the Developing World, Swedish International Development Cooperation Agency and National Research Foundation.

**Keywords:** *Aspergillus* sp. | methicillin-resistant *Staphylococcus aureus* | *Meyerozyma guilliermondii* | molecular docking | penicillin-binding protein 2a (PBP2a) | *Penicillium* sp.

## Abstract

The genus *Grewia* are well-known for their medicinal properties and are widely used in traditional remedies due to their rich phytochemical composition and potential health benefits. This study isolated and characterized five endophytic fungi from *Grewia lasiocarpa* E. Mey. Ex Harv. and evaluated their in vitro antibacterial and antioxidant activities. Five [*Aspergillus fumigatus* (MK243397.1), *A. fumigatus* (MK243451.1), *Penicillium raistrickii* (MK243492.1), *P. spinulosum* (MK243479.1), *Meyerozyma guilliermondii* (MK243634.1)] of the 22 isolated endophytic fungi had inhibitory activity (62.5–1000 µg/mL) against methicillin-resistant *Staphylococcus aureus* (MRSA). The antioxidant activities were 66.5% and 98.4% for 2,2-diphenyl-1-picrylhydrazyl (DPPH) and ferric ion reducing antioxidant power (FRAP), respectively. In silico evaluation of the phytochemicals of the extract (containing majorly *n*-hexadecanoic acid) was performed against penicillin-binding protein 2a (PBP2a) implicated in the broad clinical resistance of MRSA to conventional beta-lactams. Molecular docking and molecular dynamic simulation analyses revealed that the phytosterol constituents of the extract, especially dehydroergosterol (−46.28 kcal/mol), had good stability (4.35 Å) and compactness (35.08 Å) with PBP2a relative to the unbound PBP2a and amoxicillin-PBP2a complex during the 100 ns simulation period, reinforcing them as putative leads that may be developed as viable alternatives to beta-lactams against infections caused by MRSA. However, the prediction that dehydroergosterol lacks oral bioavailability with poor water solubility suggests that it could benefit from structural optimization for improved druggability. Hence, isolating and derivatizing dehydroergosterol for subsequent evaluation against PBP2a in vitro and in vivo is highly recommended.

**Abbreviations:** A, active; BA, binding affinity; BS, bioavailability score; C, carcinogenicity; CY, cytotoxicity; CYP, cytochrome; GI-A, gastrointestinal absorption; H, hepatotoxicity; HB-A, hydrogen bond acceptor; HB-D, hydrogen bond donor; I, inactive; IM, immunotoxicity; L, low; LD, lethal dose; Log Po/w, partition coefficient; M, mutagenicity; MS, moderately soluble; MW, molecular weight; N, no; Pgp, permeability glycoprotein substrate; PS, poorly soluble; RT-B, rotatable bond; S, soluble; SA, synthetic accessibility; TC, toxicity class; VS, very soluble; WS, water solubility; Y, yes.

This is an open access article under the terms of the [Creative Commons Attribution-NonCommercial](https://creativecommons.org/licenses/by-nc/4.0/) License, which permits use, distribution and reproduction in any medium, provided the original work is properly cited and is not used for commercial purposes.

© 2025 The Author(s). *Chemistry & Biodiversity* published by Wiley-VHCA AG.

## 1 | Introduction

Despite advances in modern medicine, infectious diseases remain a leading cause of death in tropical countries [1]. The rise of antibiotic-resistant strains, including methicillin-resistant *Staphylococcus aureus* (MRSA), underscores the urgent need for new antibacterial agents [2]. Medicinal plants continue to gain therapeutic attention due to their long-term uses among local communities to treat symptoms of diseases. Although plant secondary metabolites have been explored in drug discovery, existing evidence indicates that they often harbour several microorganisms, collectively known as endophytes, which remain an untapped natural source for drug discovery [3]. Thus, exploring endophyte-derived natural products might increase the likelihood of finding novel compounds in the treatment of multidrug-resistant microorganisms.

Microorganisms, including actinomycetes, bacteria and fungi, inhabit both plants and animals, where they can be either pathogenic or beneficial [4]. Among these, endophytes are unique class of microorganisms that reside within plant tissues without causing harm, establishing a mutualistic relationship with their host [5]. Endophytes are ubiquitous in nature, present in most plants, with an estimated 300 000 plant species hosting them [6]. The surge in the study of endophytic fungi is driven by their potential to produce diverse natural products, some of which have significant pharmaceutical and industrial applications [6, 7]. Endophytic fungi provide various benefits to their host plants, including protection against herbivores and pathogens and aiding in adaptation to environmental stressors in exchange for nutrients [8]. These fungi produce a plethora of metabolites, many of which have demonstrated antibacterial, anticancer, antidiabetic, antifungal, antioxidant, antiviral and antileishmanial activities [9]. Despite the extensive benefits and potential applications of endophytes, there is paucity of information on those associated with *Grewia lasiocarpa* E. Mey. Ex. Harv. It is an indigenous Southern African plant which has remained understudied, likely due to its endemic nature [10]. Notably, *Aspergillus fumigatus* and *Alternaria alternata* are the only endophytic fungi previously isolated from the genus *Grewia* [11], necessitating the need to further explore the genus. *G. lasiocarpa* has been documented in traditional medicine, especially in formulations used to address complications during child birth [12]. Recent research has identified bioactive metabolites in the leaves and stem bark of *G. lasiocarpa* [13]. Endophytes associated with this plant may serve as abundant sources of novel phytochemicals with significant therapeutic potential.

The survival of bacteria depends on the integrity of their cell walls, which are synthesized by the penicillin-binding proteins (PBPs). *S. aureus* possesses four inherent PBPs (PBP1, PBP2, PBP3 and PBP4) [14]. However, *mecA*-encoded PBP2a (PBP2a) is commonly found in MRSA and confers resistance to most conventional beta-lactam antibiotics. Due to the essential role of PBP2a in MRSA cell wall synthesis, which is crucial for the survival of the organism, PBP2a represents an excellent drug target for the identification of promising alternative beta-lactams [14]. Hence, identifying active modulators of PBP2a from endophytes such as those of *G. lasiocarpa* might help in the fight against infections caused by MRSA. Hence, this study isolated, characterized and evaluated the antioxidant and

antibacterial properties of secondary metabolites of fungal endophytes in the leaves and stem bark of *G. lasiocarpa*. Although in vitro study is an important phase in drug discovery, computational studies such as molecular docking and molecular dynamics (MD) simulation allow for rapid identification of lead compounds in plants [15]. In addition to metabolite profiling and evaluation of the antibacterial antioxidant properties in vitro, the lead antibacterial compounds in endophytic extract of *G. lasiocarpa* were computationally profiled against PBP2a of MRSA.

## 2 | Materials and Methods

### 2.1 | Collection of Plant Material

Fresh and healthy plant materials (leaves and stem bark) of *G. lasiocarpa* were used for the isolation of the endophytic fungi. The plant was taxonomically identified and authenticated by Dr. Syd Ramdhani, the herbarium curator for the University of KwaZulu-Natal (UKZN), South Africa. A voucher specimen denoted as 'Nneka 002' was deposited at the UKZN Herbarium. The plant materials were collected from the Umdoni Trust Park, Pennington, in winter and temporarily preserved in sterile airtight polythene bags to retain and increase humidity stored in an icebox. The fresh materials were stored at 4°C and processed for the isolation of the endophytic fungi within 72 h after collection.

### 2.2 | Preparation of Culture Media for Isolation of Endophytic Fungi

#### 2.2.1 | Chemically Synthesized Standard Culture Media

The media were used singly and supplemented with plant-based aqueous extracts at different concentrations to observe the fungal diversity that will be ensued. The fresh leaves and stem bark of *G. lasiocarpa* were washed under running water and pulverized using a Waring blender at a 1:10 (w/v) ratio of plant material to distilled water. To obtain the plant extracts, the slurry was filtered using a clean and sterile muslin cloth. Each of the plant extracts was further diluted with distilled water (v/v) to concentrations of 5%, 2.5% and 1.25% to formulate the malt extract agar (MEA), potato dextrose agar (PDA) and bacteriological agar (BA) plant-based agar cultures. Three commercial media were used, namely, MEA (pH 4.7), PDA (pH 5.6) and BA (pH 7.1) (BioLAB), all made up to 250 mL of sterile distilled water and autoclaved at 121°C for 15 min. All the media were supplemented with 10 mg/mL ampicillin and streptomycin 50 mg/mL.

### 2.3 | Isolation of the Endophytic Fungi

The method of Strobel and Daisy [16], with slight modifications, was used for the isolation of the endophytic fungi from the leaves and stem bark of *G. lasiocarpa*. The leaves and stem bark were washed gently, under running tap water for about 2 min, followed by another four times rinse. The plant organs were dried using an absorbent paper and cut with a sterile scalpel into small pieces of ca. 2–10 mm<sup>2</sup>. For the leaves, the margins were discarded, and leaf pieces excised as described by Luginbühl [17], three

pieces from the lamina, two from the adjacent sides between the mid-vein and the margin, and one from midway between the petiole and the leaf base. For the stem bark, the photosynthetic segments were used. The cut segments of the leaves and stem bark were treated separately in pre-cleaned 250 mL beakers. First, the tissues were treated with 0.1% Tween 20 (wetting agent dispersant) for 5 min, and then an agitated sequential successive immersion was carried out using 75% (v/v) ethanol for 5 min to remove surface hydrophobic matters, dehydrate the pubescent on the surfaces and allow easy infiltration of the sterilizing agent. The tissues were then transferred to a beaker containing 2.5% aqueous solution of sodium hypochlorite (NaOCl/NaClO) for 10 min to eliminate the remaining epiphytic microorganism(s) present. Thereafter, re-dipped in 75% ethanol for 5 min and finally rigorously rinsed thrice in sterile distilled water for 2 min to remove residual sterilants and left to dry in sterile Petri dishes under aseptic conditions in the hood to prevent air contamination of the tissues [18]. The effectiveness of the surface sterilization was checked by plating aliquots of about 0.1 mL of water from the last rinse on each of the representative media used for the experimental procedure [19]. The segments were placed on the prepared solid agar. Three or more excised tissues were plated directly and evenly spaced on sterilised Petri dishes (9 cm diameter) on each of the prepared media, with a uniform thickness of 4 mm. The plates were sealed with parafilm and incubated in the dark at 25°C–30°C. For the negative control, all steps mentioned above were carried out without the surface sterilization of cut segments and imprints of three randomly selected leaves, and stem bark was made on each representative agar plate. A regular 3-day interval examination for emerging fungal hyphae from the edges of plant tissues was carried out. To obtain pure cultures, that is, morphologically similar hyphal tips (mycelia), the fungal colonies were isolated and passed through rounds of subculture on the same media without antibiotic because antimicrobial agents inhibit certain fungi. The last subculture was obtained on PDA media supplemented with antibiotics as above.

### 2.3.1 | Morphological Identification of Endophytic Isolates

Identification of isolated conidia-producing strains was carried out using prior knowledge and microscopic examination of the spores with *lactophenol* cotton blue stain for light microscopy. Stereomicroscopy was used to view the macro-morphology of the endophytic fungi [20].

### 2.4 | Cultivation and Secondary Metabolite Extraction

A regular examination for emerging fungal hyphae from the edges of plant tissues was conducted at 3-day intervals. To obtain pure cultures of morphologically similar hyphal tips (mycelia), the fungal colonies were isolated and subjected to multiple rounds of subculturing on the same media without antibiotics, as certain fungi are partially inhibited by antimicrobial agents. The final subcultures of actively growing pure fungal cultures were subcultured on PDA at 25°C ± 2°C supplemented with antibiotics at concentrations of 10 mg/mL ampicillin and 50 mg/mL streptomycin for 5 days [14]. Each of these selected pure fungal

endophytes was inoculated on cooked rice medium (10 g of rice in 20 mL of peptone water [0.5% peptone and 0.3% NaCl]) by placing agar blocks of actively growing pure cultures (3 mm in diameter), in a 250 mL Erlenmeyer flask, to ferment for 30 days at room temperature in the dark [21].

This transfer was done in triplicates, whereas for the negative control, an Erlenmeyer flask with the same volume of medium but without the inoculum was also treated as described above.

Thereafter, the growth phase was finally arrested by the addition of 50 mL of ethyl acetate into each biomass contained in the Erlenmeyer flask and agitated gently in a rotary shaker (180 rpm, incubated at 27°C ± 3°C on a Labcon flatbed shaker for 72 h). To obtain the intracellular metabolites, the biomass and fungal extract mixtures were transferred into a separating funnel, with the addition of 50 mL of distilled deionised water to remove traces of starch, mixed vigorously for 10 min and allowed to stand. The organic layer was used as the fungal extract, whereas the extracted mycelia (cell fragments) obtained were discarded. The two phases—ethyl acetate and medium (water phase)—were transferred to centrifuge tubes and separated by centrifuging at 6000 rpm for 20 min at 17°C. The resulting organic layer was evaporated to produce the ethyl acetate-concentrated extracts, weighed and stored in glass vials.

## 2.5 | Chemical Composition of Extracts

### 2.5.1 | Fourier Transform Infrared Spectroscopy (FTIR) Analysis

The spectra of the ethyl acetate extracts of the 22 endophytic fungi were obtained using FTIR spectroscopy on a Perkin-Elmer FTIR using spectrum software version 6.1. The data of infrared absorbance of a minute amount of the dried extract were recorded over the wave number range of 4000–400 cm<sup>−1</sup> with a 4 cm<sup>−1</sup> resolution at 25°C ± 2°C [22].

### 2.5.2 | Gas Chromatography–Mass Spectrometric (GC–MS) Analysis

The GC–MS analysis of the ethyl acetate extracts of *G. lasiocarpa* [GLANA (1–5)], with antibacterial properties, was conducted using a GCMS-QP2010 Plus Shimadzu instrument coupled with fitted a capillary chromatographic column of 30 m × 0.25 mm ID × 0.25 µm film thickness of 5% phenylmethylsiloxane. The instrument was set to an initial temperature of 50°C, maintained for 1.5 min, then increased to 200°C at a rate of 4°C min<sup>−1</sup> and increased up to 300°C at the rate of 10°C min<sup>−1</sup> held for 7 min. The injector and interface temperatures were 240°C and 220°C, respectively. The helium flow rate was 1.2 mL min<sup>−1</sup>, and 0.4 µL of each of the extracts were solubilised and diluted (1/100) in ethyl acetate (≥99%, GC grade, Sigma-Aldrich). The solution was further filtrated using a 0.22 µm filter, which was injected into the ‘split’ mode system. The mass spectral scan mode range was 40–500 *m/z*, with a total running time of 37 min. The compounds were identified by comparing their retention times and mass spectra with the National Institute of Standards and Technology, Washington, DC, USA, spectral database [13a].

## 2.6 | In Vitro Antibacterial Assay

The in vitro antibacterial activity of the ethyl acetate extracts of all 22 endophytic fungi was screened against six pathogenic bacteria [two Gram-positive: MRSA (ATCC BAA-1683), *S. aureus* (ATCC 25923) and four Gram-negative: *Escherichia coli* (ATCC 25922), *Pseudomonas aeruginosa* (ATCC 27853), *Klebsiella pneumoniae* (ATCC 314588) and *Salmonella typhimurium* (ATCC 14026)] using the agar well diffusion method described by Perez [23], with slight modifications. The strains were maintained in 75% glycerol at  $-80^{\circ}\text{C}$ . Briefly, the extracts were dissolved in 10% dimethyl sulphoxide using five dilutions of 1000, 500, 250, 125 and  $62.5\text{ }\mu\text{g/mL}$ , whereas the standard drugs were  $10\text{ }\mu\text{g/mL}$  of gentamicin (Gram-negative) and streptomycin (Gram-positive), which were used as the positive controls. The bacteria were standardised at 625 nm to an OD concentration of  $1 \times 10^8$  to  $1 \times 10^9$  cfu/mL and seeded on Müller–Hinton (MH) sterile agar plates with a sterile cotton swab. In each of the plates, six wells (6 mm diameter) were made using a sterile cork borer, and then  $100\text{ }\mu\text{L}$  of the five dilutions and the standard were added separately to the well. The plates were incubated at  $36^{\circ}\text{C}$  for 18–24 h, and the diameter of the zones of inhibitions was measured in mm. The tests were conducted in triplicates, and data were expressed as mean  $\pm$  standard deviation.

## 2.7 | In Vitro Antioxidant Assay

The radical scavenging ability of the extracts was evaluated using 2,2'-diphenyl-1-picrylhydrazyl (DPPH) as described by Braca et al. [24]. In triplicates, duplicates of  $30\text{ }\mu\text{L}$  of the chemical, ranging in concentration from 15 to  $240\text{ }\mu\text{g/mL}$ , were pipetted into a 96-well microplate. Thereafter,  $150\text{ }\mu\text{L}$  of  $0.3\text{ mM}$  DPPH solution were added to each well and incubated for 30 min at  $25^{\circ}\text{C}$  in the dark. The absorbance was measured at 517 nm, and the free radical scavenging activity was expressed as a percentage of the free radical's inhibition. The standard utilised was ascorbic acid. Plotting the percentage inhibition against the concentration logarithmic scale allowed for the determination of the  $\text{IC}_{50}$  from the inhibition curves. The following formula was used to determine the scavenging ability of the pure compound:

$$\text{DPPH scavenging activity (\%)} = \left[ \frac{(\text{Abs}_{\text{control}} - \text{Abs}_{\text{sample}})}{\text{Abs}_{\text{control}}} \right] \times 100$$

where  $\text{Abs}_{\text{control}}$  is the absorbance of DPPH and methanol, and  $\text{Abs}_{\text{sample}}$  is the absorbance of DPPH radical + sample (compound or standard).

Ferric reduction activity potential (FRAP) of the extracts was measured as described by Oyebo et al. [25]. Briefly,  $50\text{ }\mu\text{L}$  of the pure product at a concentration range of 15– $240\text{ }\mu\text{g/mL}$  were mixed with  $100\text{ }\mu\text{L}$  of 1% potassium ferricyanide and  $50\text{ }\mu\text{L}$  of  $0.2\text{ M}$  sodium phosphate buffer (pH 6.6). This was followed by  $50\text{ }\mu\text{L}$  of 10% trichloroacetic acid,  $50\text{ }\mu\text{L}$  of distilled water, and  $10\text{ }\mu\text{L}$  of  $0.1\%$  iron(III) chloride ( $\text{FeCl}_3$ ) added to each well of the microplate and incubation at  $50^{\circ}\text{C}$  for 30 min. The absorbance was measured at 700 nm, and the results were calculated using the method to show the fraction of the absorbance for the extracts to that of gallic acid:

$$\% \text{ Inhibition} = (\text{Abs of sample} / \text{Abs of Gallic acid}) \times 100$$

where Abs is the absorbance.

## 2.8 | Isolation and Molecular Identification of the Fungal Genomic DNA

The five fungal cultures with antibacterial activities were grown on PDA and incubated at  $35^{\circ}\text{C}$  for 24–48 h. The deoxyribonucleic acid (DNA) of the endophytic fungi was extracted using the ZR Soil Microbe DNA MiniPrep kit (Zymo Research) according to the manufacturer's instructions and used as a template for the polymerase chain reaction (PCR) assay.

### 2.8.1 | Detection and Confirmation of the Endophytic Fungal DNA (GLANA 1-5) by PCR

The Universal Internal Transcribed Spacer (ITS) primers 4 and 5 (Table S1) were used to amplify the ITS fungal region, following PCR of the five selected endophytic fungi. Each  $25\text{ }\mu\text{L}$  PCR assay mixture consisted of  $2\text{ }\mu\text{L}$  DNA solution,  $8.5\text{ }\mu\text{L}$  of RNA nuclease-free water,  $12.5\text{ }\mu\text{L}$  of PCR master mix and  $1\text{ }\mu\text{L}$  of each primer. Amplification of the partial sequence of the 18S rDNA genes was performed in a T100 Thermal Cycler (Biorad, USA) under the following conditions: initial denaturation at  $95^{\circ}\text{C}$  for 2 min, 25 cycles of denaturation at  $95^{\circ}\text{C}$  for 30 s, annealing at  $53^{\circ}\text{C}$  for 45 s and elongation at  $72^{\circ}\text{C}$  for 8 min. A final elongation step was performed at  $72^{\circ}\text{C}$  for another 8 min.

The amplified DNA fragments of the five endophyte samples were analysed by electrophoresis on a 1.5% agarose gel (SeaKem Gold agarose (FMC BioProducts)), and the products were visualised after staining the gel with ethidium bromide ( $0.5\text{ }\mu\text{g/mL}$ ) using the Chemigenius Bioimaging System (Syngene, England). This analysis revealed the purity and the length of the amplicons (Figure S1). The concentration of the extracted fungal DNA was determined using the NanoDrop 1000 spectrophotometer. The sequenced products as obtained from Inqaba (Inqaba Biotechnical Industries (Pty) Ltd., South Africa) were aligned with DNA sequences in GenBank database using BlastN programme Basic Local Alignment Search Tool (BLAST) (<http://blast.ncbi.nlm.nih.gov/Blast.cgi>) [26].

### 2.8.2 | Phylogenetic Analysis

The endophytic fungi sequences were deposited in National Center for Biotechnology Information (NCBI) and were given accession numbers. The phylogenetic analysis was carried out by comparing several DNA sequences from the BlastN result in Molecular Evolutionary Genetics Analysis version 7 (MEGA7) software by neighbour-joining tree method [27].

## 2.9 | Computational Analysis

### 2.9.1 | PBP2a Acquisition, Optimization and Identification of Active Sites

The experimental crystal structure of PBP2a from *S. aureus* (PDB ID: 6H5O) was sourced from the Protein Data Bank (PDB) (<https://www.rcsb.org>). This structure was refined using UCSF



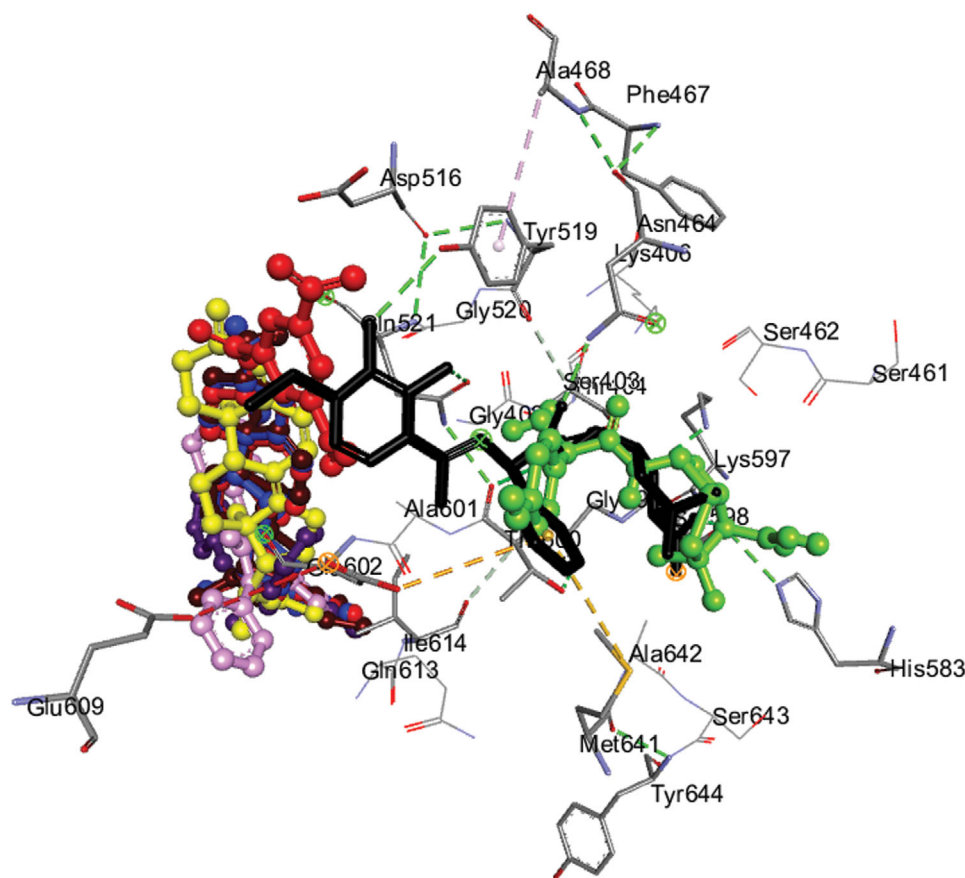


**FIGURE 1** | Docking protocol validation via superimposition of the docked top-hit compounds with the experimental native inhibitor at the active sites of 6H5O. The docked experimental inhibitor (black), reference standard amoxicillin (green), and top-hit compounds [triphenyl phosphate (purple), ergosta-4,6,8 (yellow), ergosterol (blue),  $\beta$ -sitosterol (brown), and dehydroergosterol (red), 4-azaphenanthrene (pink)] all had an RMSD of 3.0 Å from the experimental native inhibitor suggesting partial binding orientation of the docked compounds and the experimental native inhibitors.

Chimera v1.15, which involved removing water molecules and nonstandard amino acids. Subsequently, the  $x$ - $y$ - $z$  coordinates and active site amino acid residues were defined using Discovery Studio version 21.1.0, in accordance with previously reported methods and validated through literature [28].

## 2.9.2 | Ligand Acquisition, Preparation and Molecular Docking at the Active Site of PBP2a

The compound library and amoxicillin were sourced from PubChem (<https://pubchem.ncbi.nlm.nih.gov/>). Prior to molecular docking, the ligands (library of compounds and amoxicillin) were optimized using the Open Babel tool in Python Prescription (PyRx) v.0.9.5 by adding Gasteiger charges. Molecular docking was performed at the active site of PBP2a using the AutoDock Vina plug-in on PyRx v.0.9.5. The active site was targeted by selecting critical residues with grid box coordinates matching the  $x$ - $y$ - $z$  coordinates obtained from Discovery Studio. The top six compounds with the highest negative docking scores were identified, and the docking complex with the best conformation for each ligand–protein interaction was saved in PDB format for further MD simulation. Docking conformations were validated using superimposition techniques, with the root mean square deviation (RMSD) calculated for the top six docked compounds and amoxicillin against the native inhibitor of PBP2a [29], with

the RMSD calculated for the top six docked compounds and amoxicillin against the native inhibitor of PBP2a (Figure 1).

## 2.9.3 | MD Simulations and Post-Simulation Analysis of Top Six Compounds

A 100-ns MD simulation of each of the resulting complex for the top six compounds, amoxicillin and apo-PBP2a was performed using the AMBER 18 package of the in-house Programme HEAL1361 of the Centre for High Performance Computing (CHPC), Cape Town, South Africa, employing the FF18SB variant of the AMBER force field. Atomic partial charges of the ligands were created using the ANTECHAMBER tool with the general AMBER force field (GAFF) and restrained electrostatic potential (RESP) approaches. The AMBER LEaP module assigned the protonation states, ensuring accurate assignment for each amino acid residue using  $\text{Na}^+$ , hydrogen atoms and  $\text{Cl}^-$  counter ions. Residue numbering from 1 to 658 was performed, and the systems were immersed in an orthorhombic box of TIP3P water molecules, ensuring that each atom was within 8 Å of any box edge.

Each system, including the top hit compounds, amoxicillin and apo-PBP2a, underwent initial equilibrium (2000 steps) with a 500 kcal/mol restriction potential. This was followed by 990 steps using the steepest descent technique and conjugate gradient

method, and then 990 steps of unrestricted minimization using the conjugate gradient approach [30]. Heating simulations were performed over 50 ps, gradually increasing from 0 to 300 K while maintaining a constant number of atoms and volume, with a harmonic constraint of 10 kcal/mol on solutes and a collision frequency of 1.0 ps.

Each system was equilibrated for approximately 500 ps at a constant temperature of 300 K. The SHAKE method was used to restrict hydrogen bonds, with each system employing a randomized seeding and a 2 fs step size, corresponding to the isobaric-isothermal ensemble (NPT). Simulations maintained a constant pressure (1 bar) and temperature (300 K), using a Langevin thermostat to control the collision frequency at 1.0 ps and a pressure-coupling constant of 2 ps. Post-simulation analysis involved collecting system coordinates and trajectories using the PTRAJ module and analysing RMSD, root mean square fluctuation (RMSF), radius of gyration (ROG) and solvent accessible surface area (SASA) with the CPPTRAJ module, plotting the results with Origin v 6.0 [30].

Binding free energy ( $\Delta G_{\text{bind}}$ ) was determined using 120 000 snapshots (at 1.0 ps intervals) from the 120 ns MD simulation trajectory, using the MMGBSA technique and the following equations:

$$\Delta G_{\text{bind}} = G_{\text{complex}} - (G_{\text{receptor}} + G_{\text{ligand}}) \quad (1)$$

$$\Delta G_{\text{bind}} = -TS + (G_{\text{sol}} + E_{\text{gas}}) \quad (2)$$

$$E_{\text{ele}} + E_{\text{int}} + E_{\text{vdw}} = E_{\text{gas}} \quad (3)$$

$$-(G_{\text{GB}} - G_{\text{SA}}) = G_{\text{sol}} \quad (4)$$

$$\gamma \cdot \text{SASA} = G_{\text{SA}} \quad (5)$$

where  $E_{\text{gas}}$  is the gas-phase energy,  $E_{\text{int}}$  is the internal energy,  $E_{\text{ele}}$  is the Coulomb energy,  $E_{\text{vdw}}$  is the van der Waals energy,  $G_{\text{sol}}$  is the solvation-free energy from polar state,  $G_{\text{GB}}$  is the solvation-free energy from the polar and non-polar states,  $S$  is the total entropy, and  $T$  is the temperature.

#### 2.9.4 | Pharmacokinetic and Physicochemical Prediction of Top Six Compounds

The pharmacokinetics, physicochemical properties and drug-like characteristics of the top six compounds were predicted using their SMILES (Simplified Molecular Input Line Entry System) representations through the SwissADME web tool (<http://swissadme.ch/index.php>). These predictions were subsequently validated with the Molinspiration toolkit (<https://www.molinspiration.com/cgi-bin/properties>). Additionally, the toxicity properties of the compounds were assessed using the Protox II web server ([https://tox-new.charite.de/protox\\_II/](https://tox-new.charite.de/protox_II/)).

## 3 | Results and Discussion

### 3.1 | Morphology of the Selected Endophytes

A total of 573 endophytic fungi were isolated from 309 segments of the fresh, healthy leaves and stem bark of *G. lasiocarpa*. This generated 22 relatively common endophytic fungi that were morphologically selected and isolated from the leaves and stem bark (Figure 2A–E).

### 3.2 | Antibacterial Activity of the Endophytic Fungal Extracts

In this study, out of the 22 endophytic fungi extracts analysed, 17 showed no inhibitory effect on the tested bacterial strains. Six clinical isolates of human pathogenic bacteria were tested, and four endophytes exhibited a bacterial-specific activity against MRSA, and only GLANA3 extract showed an inhibitory effect against *S. aureus* (Table 1). The sensitivity of the test organisms to the GLANA1-5 extracts was measured by zones of inhibition with a range between 17.3 and 6.5 mm. The fungal endophyte (GLANA1) gave the maximum inhibition zone (17.3 mm) against MRSA. The extracts significantly inhibited the growth of MRSA (ATCC BAA-1683) but were not effective against *P. aeruginosa* (ATCC 27853), *S. typhimurium* (ATCC 14026), *K. pneumonia* (ATCC 314588) and *E. coli* (ATCC 25922). The GLANA3 extract showed significant antibacterial activity against *S. aureus* (ATCC 25923). This implies that the presence of one or a group of phytocompound(s) may have influenced this inhibition against *S. aureus*. Generally, the strain bacterial inhibition specificity is in correlation with a previous finding [13a], where the highest inhibition (30%) was with the drug-resistance bacteria (MRSA and *S. aureus*), thus confirming that the mutually symbiotic relationship exhibited by endophytic fungi with their host plant facilitates the biosynthesis of similar phytocompounds/derivatives or phytocompounds with similar antibacterial properties.

The antibacterial activity of endophytic fungi isolated from plants has also been reported [31]. Although GLANA1 and GLANA2 are derived from the same species, their differing antibacterial activities suggest that molecular variations between the two may lead to distinct phytometabolite production. The hexane, methanol and chloroform extracts and an isolated compound (lupeol) from *G. lasiocarpa* have been observed to have antibacterial activities against some clinical bacterial strains [13a, 32]. This suggests that the extracts from GLANA1 and 2 either lack bioactive phytocompounds or the concentrations used were relatively low. Consequently, the observed bacterial inhibitions by the five extracts are considered significant.

### 3.3 | Phytochemical Profile of the Ethyl Acetate Extracts

#### 3.3.1 | FTIR Spectra of Fungal Endophytes

The extracts of the 22 fungal endophytes were subjected to FTIR analysis, which revealed the presence of alkanes (C–H stretch) and unsaturated aldehyde groups (C=O) which showed as the major collective peaks at 2908–2838 and 1710–1685  $\text{cm}^{-1}$ ,

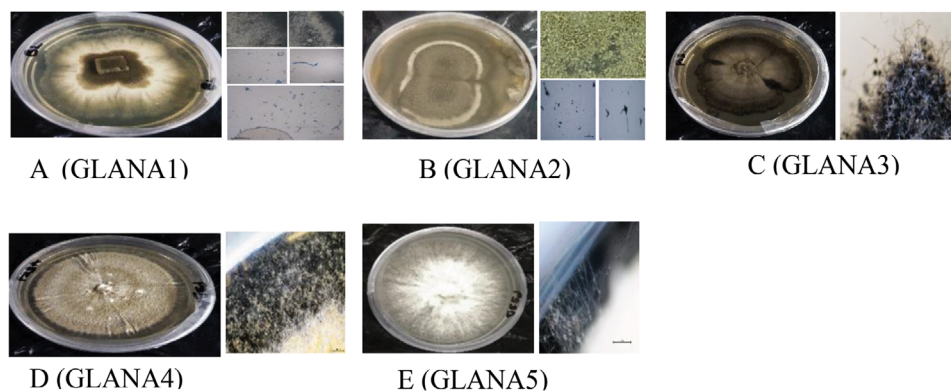


**FIGURE 2** | (A–E) Morphology of the five endophytic fungi from the leaves and stem bark of *Grewia lasiocarpa* E. Mey. Ex Harv. with antibacterial activity. GLANA1 = *Aspergillus fumigatus* (MK243397.1), GLANA2 = *Aspergillus fumigatus* (MK243451.1), GLANA3 = *Penicillium spinulosum* (MK243479.1), GLANA4 = *Penicillium raistrickii* (MK243492.1) and GLANA5 = *Meyerozyma guilliermondii* (MK243634.1).

**TABLE 1** | Antibacterial activity (zone of inhibition, diameter in mm) of the GLANA (1–5) ethyl acetate extracts of endophytic fungi from *Grewia lasiocarpa* E. Mey. Ex Harv. leaves and stem bark.

Bacterial strain: methicillin-resistant <i>Staphylococcus aureus</i>						
Fungal strain	1000 µg/mL	500 µg/mL	250 µg/mL	125 µg/mL	62.5 µg/mL	Control 10 µg/mL
GLANA1	17.33 ± 1.15	16.33 ± 1.15	10.33 ± 3.51	6.50 ± 0.50	6.50 ± 0.00	12.67 ± 2.52
GLANA2	16.67 ± 2.52	10.83 ± 1.76	6.50 ± 0.00	R	R	13.00 ± 3.46
GLANA3	17.67 ± 1.53	12.330 ± 1.53	8.33 ± 1.15	6.67 ± 0.29	6.50 ± 3.75	17.67 ± 4.04
GLANA4	11.00 ± 0.00	10.00 ± 0.00	6.50 ± 0.00	6.50 ± 0.00	6.50 ± 0.00	21.67 ± 1.15
GLANA5	6.50 ± 0.00	6.50 ± 0.00	6.50 ± 0.00	6.50 ± 0.00	6.50 ± 0.00	18.33 ± 2.08
Bacterial strain: <i>Staphylococcus aureus</i>						
GLANA3	15.00 ± 1.00	12.33 ± 0.58	11.00 ± 0.00	8.67 ± 0.58	7.83 ± 1.26	18.00 ± 1.73

Note: All other extracts showed no inhibitory activity against all the tested six bacterial strains. ( $n = 3$ ): Control: streptomycin. GLANA1 = *Aspergillus fumigatus* (MK243397.1), GLANA2 = *Aspergillus fumigatus* (MK243451.1), GLANA3 = *Penicillium spinulosum* (MK243479.1), GLANA4 = *Penicillium raistrickii* (MK243492.1), and GLANA5 = *Meyerozyma guilliermondii* (MK243634.1).

Abbreviations: MRSA, methicillin-resistant *Staphylococcus aureus*; R, resistant.

respectively (Figure S2). The FTIR overlay of the five endophytic fungi (GLANA1–5) was also done (Figure 3). A comparison of the peaks did not show a significant difference (Figure S2).

The FTIR analysis revealed the presence of lipids, of which fatty acids are components, and other metabolites in the extracts of GLANA1–5. These fatty acids have characteristically strong absorption bands arising from C–H stretching vibrations of lipids around 3100–2800  $\text{cm}^{-1}$  [33]. The metabolites such as phenol, 3,5-bis(1,1-dimethylethyl), squalene, hexadecanoic acid and *cis*-vaccenic acid are present in the ethyl acetate extracts, which have diverse biological activities such as anti-inflammatory, immunosuppressant, antimicrobial and anticancer [34]. All the extracts are rich in fatty acids and fatty acid-derived compounds. Although both flavonoids and phenols are present in the extracts, the antioxidant activity was significantly low. This may be due to the low concentration of these compounds and the high percentage of other non-antioxidant compounds. In addition, phenolic compounds are good antifungal and antibacterial agents [35].

### 3.3.2 | GC–MS Profile

The results of the GC–MS analysis of the ethyl acetate extract of the five sequenced endophytic fungi are presented in Tables S2–S6. Hexadecanoic acid, ethyl ester, methyl 8-heptadecenoate, griseofulvin and oxacycloheptadec-8-en-2-one, (8Z)3 were amongst the major compounds in the five fungal extracts. Most of the extracts were found to have a high concentration of *n*-hexadecanoic acid, recognized for its antibacterial properties. Additionally, the GC–MS analysis revealed this compound as a key ingredient present in all five extracts demonstrating antibacterial activity. The high concentration of this long-chain saturated fatty acid might contribute to the inhibitory activity against Gram-positive bacteria [36]. The presence of *n*-hexadecanoic acid has also been reported in *Aspergillus* species [37]. Additionally, the high percentage of griseofulvin in *Penicillium raistrickii* (MK243492.1) suggests it as a potential source of an antifungal agent [38], warranting further investigation into its antifungal properties. Therefore, these endophytic fungi present promising alternatives for the large-scale production of antibiotics and antifungal drugs. However, endophytes may

exhibit different behaviours in a bioreactor, including variations in the production of bioactive constituents. Phenolic compounds are broadly categorised into two, namely, flavonoids and non-flavonoids [39]. In addition, phenolic compounds are good antifungal and antibacterial agents [40].

The GC–MS results of these extracts suggest that the low antioxidant activity might be due to the chemical composition of the extracts. The query sequence of similarity values from the 18S rRNA stretch BLAST of the isolates and other phylogenetic sisters showed values of 100% identity and >99% query cover for GLANA 1–5. Therefore, using morphological and molecular genetics, GLANA 1 and 2 were identified as *A. fumigatus*, GLANA 3 as *Penicillium spinulosum*, GLANA 4 as *P. raistrickii*, GLANA 5 as *Meyerozyma guilliermondii*. The genetic divergence of the isolated endophytic fungi phylogenetic analysis suggests a slow-evolving genomic island; thus, accessory chromosomes and chromosomal rearrangements have a role to play in the observed diversity [41]. Although 22 endophytic fungi were isolated from the leaves and stem bark of *G. lasiocarpa*, only five exhibited antibacterial activities. The endophytic fungi, *A. fumigatus* (GA-L7), have also been isolated from *Grewia asiatica* L. [11c].

Furthermore, bio-active and novel compounds have been derived from *A. fumigatus* [42], *P. raistrickii* [43], *P. spinulosum* [44] and *M. guilliermondii* [45]. This may suggest that several novel compounds produced by plants endophytic fungi are yet to be discovered. However, this is the first report on the presence of *P. spinulosum*, *P. raistrickii* and *M. guilliermondii* in the genus *Grewia*, the antibacterial and antioxidant activities of the five isolates.

### 3.4 | Antioxidant Activity

Studies have explored the antioxidant potential of fungal [46] and plant metabolites with varying results [46, 47]. Certain substances from fungal strain, such as *Antrodia cinnamomea*, have demonstrated higher free radical scavenging than synthetic antioxidants, indicating their potential as antioxidants [48]. Antioxidant qualities have been shown by marine-derived fungi; in several tests, certain species showed activity that is equivalent to that of ascorbic acid [49]. Natural antioxidants for industrial use have possible sources from lignicolous fungi, especially *Ganoderma* species [50]. Not all fungal metabolites exerted appreciable antioxidant action.

The extracts exhibited an insignificant antioxidant activity compared with the standard drugs, namely, ascorbic and gallic acids (Data not shown). The highest inhibition (%) was observed in gallic acid in DPPH (66.54%) and FRAP (98.40%) assays, whereas all the fungal extracts were less than 10%. A comparison with the standards revealed that several of the extracts were not dose-dependent (Data not shown); thus, the IC<sub>50</sub> values of such were not determined. A similar observation was reported in the study on endophytic fungi from *Jatropha curcas* where they found that although some fungal strains showed promising antioxidant properties, others displayed minimal activity [51]. These findings suggest that the antioxidant potential of fungal metabolites varies considerably among species and extraction methods.

### 3.5 | Registration of Sequences

The ITS sequences from GLANA1 (derived from the leaves), GLANA2 (derived from the stem bark), GLANA3 (derived from the leaves), GLANA4 (derived from the stem bark), and GLANA5 (derived from the stem bark) were compared with GenBank database. From the morphological and molecular genetics of the five endophytic fungi, *A. fumigatus* (MK243397.1) was identified as GLANA1, *A. fumigatus* (MK243451.1) as GLANA2, *P. spinulosum* (MK243479.1) as GLANA3, *P. raistrickii* (MK243492.1) as GLANA4 and *M. guilliermondii* (MK243634.1) as GLANA5. These identifications were the closest match in a pairwise similarity to three genera (Figure 4).

### 3.6 | Phylogenetic Profile

The phenogram revealed the phylogenetic distances of fungi with homologous DNA sequences with those obtained in our study (Figure 4). These phenograms revealed that great diversity exists among the endophytes from our research and other closely related fungi sequences. However, a lower diversity (%) was observed among our five sequenced endophytic fungi (Figure 4).

### 3.7 | Molecular Docking of Metabolite of Endophytic Fungi Isolated From *G. lasiocarpa* Against the Active Site of PBP2a of *S. aureus*

Due to the effectiveness of endophytic fungi extracts on MRSA relative to other organisms in vitro, docking of all 69 profiled metabolites from the extracts was done against PBP2a. MecA-encoded PBP2a is found in MRSA, and its presence enables resistance in the organisms as they can facilitate cell wall production even after other native PBPs are inactivated [14]. In this study, the 69 profiled metabolites had docking scores ranging from −2.8 to −8.7 kcal/mol against PBP2a, with dehydroergosterol 3,5-dinitrobenzoate achieving the highest negative docking score (Table 2). Relative to amoxicillin (−7.0 kcal/mol), all the top-ranked metabolites had higher negative docking scores, suggestive of their better binding orientation and fitness at the binding pocket of PBP2a. Docking validation at the native inhibitor binding position of PBP2a (6H5O) showed that all the top-ranked compounds and amoxicillin had an RMSD value of 3.0 Å (Figure 1) from the native inhibitor of PBP2a. An RMSD of less than 2 Å indicated a comparable binding conformation [52]. Thus, the observation of 3.0 Å RMSD in this study for the docked complexes might suggest partial binding orientation as the native inhibitor of PBP2a. Moreover, the top-ranked metabolites were observed to interact with key amino acid residues such as Ser403, Ser462 and Ser602 (Figure 1), as reported in prior studies as critical for PBP2a inactivation [53].

### 3.8 | Thermodynamics Binding Free Energy of Top-Ranked Metabolites Against PBP2a

The thermodynamic binding free energy of the top six compounds against PBP2a was assessed after 100 ns MD simulation. Binding free energy measures the free energy differences between the



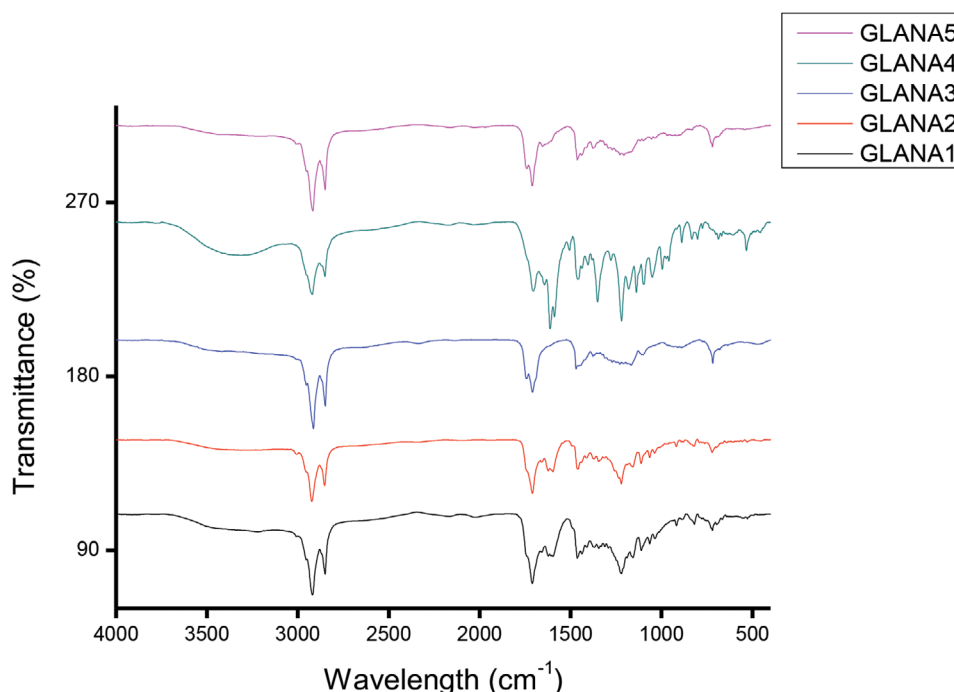


**FIGURE 3** | Overlay of the Fourier transform infrared spectroscopy (FTIR) spectra of the five-bioactivity directed selected endophytic fungi from the leaves and stem bark of *Grewia lasiocarpa* E. Mey. Ex Harv. GLANA1 = *Aspergillus fumigatus* (MK243397.1), GLANA2 = *Aspergillus fumigatus* (MK243451.1), GLANA3 = *Penicillium spinulosum* (MK243479.1), GLANA4 = *Penicillium raistrickii* (MK243492.1) and GLANA5 = *Meyerozyma guilliermondii* (MK243634.1).

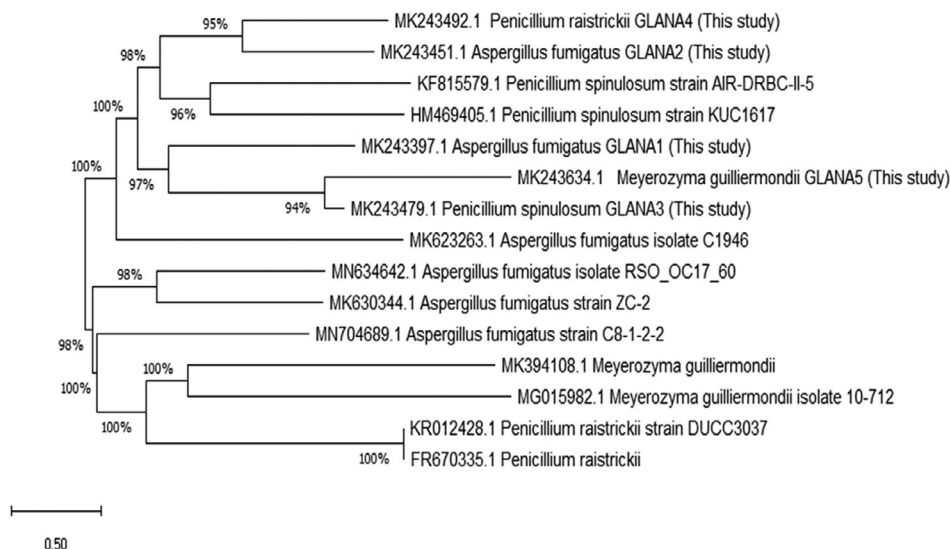


**FIGURE 4** | Phylogenetic tree depicting the genetic relationship between all five *Aspergillus fumigatus* (MK243397.1), *Aspergillus fumigatus* (MK243451.1), *Penicillium spinulosum* (MK243479.1), *Penicillium raistrickii* (MK243492.1) and *Meyerozyma guilliermondii* (MK243634.1) strains (GLANA1-5) from this study and closely related fungal DNA sequences obtained from NCBI. Bootstrap consensus tree generated by Bootstrap test phylogeny using neighbour-joining (N-J) method of MEGA 7 Software.

bound and completely unbound states during MD simulation [54]. Lower binding free energy indicates higher binding affinity of the compounds to the receptor. Among the top six compounds, dehydroergosterol,  $\beta$ -sitosterol, ergosterol, ergosta-4,6,8(14),22-tetraen-3-one and triphenyl phosphate with  $-46.28$ ,  $-46.08$ ,  $-36.07$ ,  $-24.54$  and  $-30.78$  kcal/mol, respectively, had lower binding free energy relative to the reference standard, amoxicillin ( $-21.54$  kcal/mol). This observation could suggest the

better affinity of the top-ranked compounds and most especially dehydroergosterol as modulators of PBP2a (Table 3). The binding free energy observed for dehydroergosterol, ergosterol, and  $\beta$ -sitosterol in this study is lower than that reported by prior study from the screening of all known phenolics against PBP2a (between  $-19.08$  and  $-25.61$  kcal/mol) [55], suggestive of the better potential of this class of compound (phytosterol) as modulators of PBP2a.

**TABLE 2** | Docking scores of top six metabolites from *Grewia lasiocarpa* E. Mey. Ex Harv. endophytic fungi extract against penicillin-binding protein 2a (PBP2a).

S/N	Source endophyte	Docking score (kcal/mol)	Compound
1.	GLANA2: <i>Aspergillus fumigatus</i> (MK243451.1)	−7.4	4-Azaphenanthrene, 1,2-dimethyl-4-phenylethynyl-Conformer3D_COMPOUND_CID_136370
2.	GLANA4: <i>Penicillium raistrickii</i> (MK243492.1)	−8.7	Dehydroergosterol 3,5-dinitrobenzoate Conformer3D_COMPOUND_CID_21159991
3.	GLANA4: <i>Penicillium raistrickii</i> (MK243492.1)	−7.4	$\beta$ -Sitosterol Conformer3D_COMPOUND_CID_222284
4.	GLANA4: <i>Penicillium raistrickii</i> (MK243492.1)	−7.8	Ergosterol Conformer3D_COMPOUND_CID_444679
5.	GLANA4: <i>Penicillium raistrickii</i> (MK243492.1)	−7.2	Ergosta-4,6,8(14),22-tetraen-3-one Conformer3D_COMPOUND_CID_6441416
6.	GLANA5: <i>Meyerozyma guilliermondii</i> (MK243634)	−7.1	Triphenyl phosphate Conformer3D_COMPOUND_CID_8289
	Standard reference drug	−7.0	Amoxicillin Conformer3D_COMPOUND_CID_33613

**TABLE 3** | Energy components (kcal/mol) profiles of amoxicillin (reference compound) and the top six compounds against the active site of penicillin-binding protein 2a (PBP2a).

Complex	Energy components (kcal/mol)				
	$\Delta E_{\text{vdW}}$	$\Delta E_{\text{elec}}$	$\Delta G_{\text{gas}}$	$\Delta G_{\text{solv}}$	$\Delta G_{\text{bind}}$
PBP2a_amoxicillin	−22.30 ± 7.99	−74.82 ± 26.03	−97.12 ± 28.39	75.58 ± 23.67	−21.54 ± 6.59
PBP2a_4-azaphenanthrene	−6.18 ± 9.22	−24.28 ± 32.47	−30.46 ± 39.93	26.35 ± 34.73	−4.10 ± 6.57
PBP2a_beta-sitosterol	−49.76 ± 3.06	−2.05 ± 4.50	−52.24 ± 5.16	6.15 ± 3.85	−46.08 ± 3.59
PBP2a_dehydroergosterol	−50.00 ± 7.38	−2.97 ± 2.58	−60.48 ± 8.93	14.20 ± 3.14	−46.28 ± 7.73
PBP2a_Ergosta-4,6,8	−31.77 ± 6.14	−1.08 ± 2.98	−32.86 ± 6.63	8.31 ± 3.28	−24.54 ± 5.50
PBP2a_ergosterol	−40.45 ± 4.60	−5.99 ± 6.59	−46.45 ± 8.65	10.37 ± 5.29	−36.07 ± 5.07
PBP2a_Triphenyl phosphate	−36.29 ± 3.71	−16.91 ± 5.10	−53.21 ± 6.60	22.43 ± 3.71	−30.78 ± 4.32

Note:  $\Delta E_{\text{vdW}}$ , van der Waals energy;  $\Delta E_{\text{elec}}$ , electrostatic energy;  $\Delta G_{\text{gas}}$ , gas phase free energy;  $\Delta G_{\text{solv}}$ , solvation free energy; and  $\Delta G_{\text{bind}}$ , total binding free energy.

### 3.9 | Thermodynamic RMSD, ROG, RMSF and SASA of Top-Ranked Metabolites Against PBP2a

#### 3.9.1 | RMSD Analysis

The RMSD measures the average deviation between the positions of atoms in a molecule over time, relative to a reference structure [56]. In this study, the RMSD for PBP2a and its complexes with the top six compounds, as well as the standard amoxicillin, were analysed over 100 ns (Table 4). Following equilibration of all the systems at 10 ns, both the bounded and unbounded systems took different routes that influenced their average RMSD value (Figure 5). The unbound PBP2a had the highest RMSD value (6.85 Å) among all the investigated systems, suggesting significant structural changes in the apo-protein during the MD simulation. However, when complexed with the top-ranked compounds [4-azaphenanthrene (5.76 Å),  $\beta$ -sitosterol (5.53 Å), ergosterol (5.80 Å), dehydroergosterol (4.35 Å), ergosta-4,6,8 (4.84 Å) and triphenyl phosphate (3.20 Å)] and amoxicillin

(Table 4), significant reduction in RMSD value was observed, pinpointing the enhanced thermodynamic stability instigated by the top-ranked and amoxicillin in PBP2a. The lowest RMSD value was observed with PBP2a\_triphenyl phosphate (3.20 Å), suggestive of the advantage of triphenyl phosphate as modulator of PBP2a that would result in the least conformational changes following binding. Dehydroergosterol with the highest binding free energy in this study is also causing enhanced stability following binding PBP2a, which is a plus to its potential as a suitable PBP2a modulator.

#### 3.9.2 | ROG Analysis

The ROG describes the compactness of a protein structure. Lower ROG values imply a more compact structure, whereas higher values indicate a more expanded one [15]. The ROG plot showed the overall compactness and folding of all the systems relative to the reference standard and the apo-PBP2a, and all the complexes formed against PBP2a by the top six compounds were

**TABLE 4** | Average RMSD, ROG, RMSF, SASA, and intramolecular-hydrogen-bond number and distance values of the top six compounds following a 100 ns simulation at the active site of PBP2a for *Staphylococcus aureus*.

Complex	Dynamics				
	RMSD (Å)	RoG (Å)	RMSF (Å)	SASA (Å)	No. of H-bonds
PBP2a	6.85 ± 1.18	35.37 ± 0.45	2.26 ± 0.91	26786.05 ± 473	321.24 ± 12
PBP2a_amoxicillin	4.07 ± 1.15	37.57 ± 0.29	2.65 ± 1.24	27484.50 ± 458	321.44 ± 12
PBP2a_4-azaphenanthrene	5.76 ± 0.93	34.78 ± 0.49	2.52 ± 2.31	26034.48 ± 757	321.15 ± 12
PBP2a_beta-sitosterol	5.53 ± 1.96	35.23 ± 1.02	3.36 ± 1.66	25841.49 ± 553	325.43 ± 12
PBP2a_dehydroergosterol	4.35 ± 0.81	35.08 ± 0.46	2.49 ± 3.22	25511.55 ± 851	320.83 ± 11
PBP2a_Ergosta-4,6,8	4.84 ± 1.30	35.08 ± 0.57	2.80 ± 1.36	26152.64 ± 417	322.17 ± 12
PBP2a_ergosterol	5.80 ± 1.69	34.47 ± 0.95	3.07 ± 1.41	25930.48 ± 541	322.30 ± 11
PBP2a_Triphenyl phosphate	3.20 ± 0.76	35.90 ± 0.38	2.63 ± 1.29	26318.30 ± 410	318.97 ± 11

PBP2a = Penicillin-Binding Protein 2a; RMSD = Root Mean Square Deviation; ROG = Radius of Gyration; RMSF = Root Mean Square Fluctuation; SASA = Solvent Accessible Surface Area.

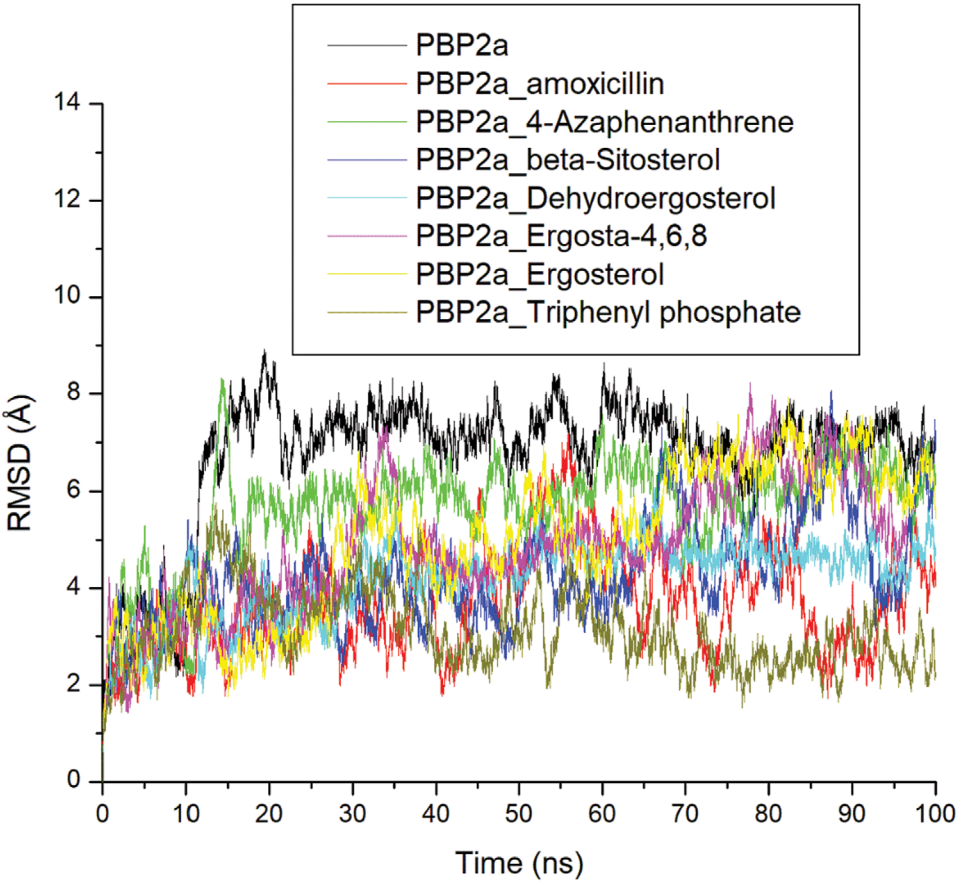


**FIGURE 5** | Comparative root mean square deviation (RMSD) plots of the alpha-carbon, the top six compounds, as well as the standard amoxicillin against the active site of penicillin-binding protein 2a (PBP2a) of *Staphylococcus aureus* over a 100 ns molecular dynamic (MD) simulation period. These figures assess the stability of these top six compounds within the active site of PBP2a, compared to the reference standard and the alpha-carbon of PBP2a itself. Overall, the comparison shows that all the compounds maintain stability with only minor fluctuations.

observed to be compact (Figure 6). Although other complexes were folding, amoxicillin-PBP2a was unfolded especially between 15 and 100 ns of the MD simulation period. Consequently, relative to the apo-PBP2a (35.37 Å), PBP2a complexed with amoxicillin (37.57 Å) had the highest ROG value, indicating

that PBP2a adopted a more expanded structure when bonded with amoxicillin. The lowest average ROG value was observed with ergosterol (34.47 Å) (Table 4), suggesting that ergosterol binding significantly tightened the PBP2a structure, making it more compact.

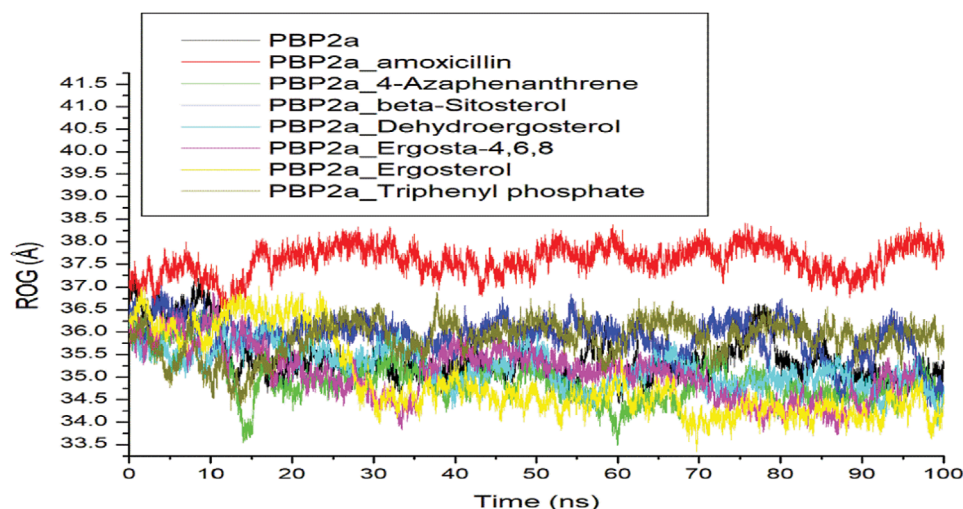


**FIGURE 6** | Comparative radius of gyration (ROG) plots of alpha-carbon, the top six compounds and standard (amoxicillin) against the active site of penicillin-binding protein 2a (PBP2a) of *Staphylococcus aureus* over 100 ns molecular dynamic (MD) simulation period. The figure reflects the overall compactness and folding of the PBP2a complexed with the top six compounds compared to that of the reference standard and the alpha-carbon of PBP2a. Relative to the reference standard and the alpha-carbon of PBP2a, all the complexes formed against PBP2a by the top six compounds were observed to be compact. Although other complexes were folding, amoxicillin-complex (red) was unfolded especially between 15 and 100 ns of the simulation period.

### 3.9.3 | RMSF Analysis

The RMSF of PBP2a complexes measures how different ligands affect the flexibility of PBP2a amino acid residues over 100 ns MD simulation [56]. Significant increases in residue movement were observed between 1 and 250 amino acid residues of PBP2a, indicating weaker intramolecular bonding within this region (Figure 7). Interestingly, the active site residues noted in Figure 1 were observed to be outside the region of higher residue fluctuations, meaning stronger intramolecular binding between adjacent residues and intermolecular binding between PBP2a residues and the top-ranked ligand and amoxicillin during the 100 ns MD simulation. PBP2a complexed with  $\beta$ -sitosterol (3.36 Å) and ergosterol (3.07 Å) had the highest RMSF values, indicating potential destabilization due to significant residue movement (Table 4). PBP2a complexed with other top-ranked compounds and amoxicillin exhibited moderate RMSF values that is <3 Å limit for good deviation indicating stable dynamic in PBP2a following binding PBP2a. Dehydroergosterol (2.49 Å) having <3 Å RMSF value also highlights its potential as modulator of PBP2a further corroborating other thermodynamic analyses conducted in this study.

### 3.9.4 | SASA Analysis

The SASA measures the surface area of a protein that is accessible to solvent [57]. Higher SASA values indicate greater surface area exposure, whereas lower values suggest more compact or buried structures. Relative to apo-PBP2a, all the complexes formed against PBP2a by the top six compounds were observed to be compact (Figure 8). Similar to the ROG findings, although other complexes maintained their folded structures, the amoxicillin-PBP2a complex exhibited unfolding, particularly during the 15–100 ns interval of the simulation period. Thus, PBP2a complexed with amoxicillin (27 484.50 Å<sup>2</sup>) had the highest SASA

value, suggesting the complex to be the most exposed to solvent with significant conformational changes. Relative to other top-ranked, dehydroergosterol when complexed with PBP2a had the lowest SASA value at 25 511.55 Å<sup>2</sup> (Table 4). This observation, while in line with other thermodynamic analysis done in this study, also shows the benefit of the compound as PBP2a inhibitor.

### 3.9.5 | Hydrogen Bond Analysis

The number of hydrogen bonds in a protein complex is an important indicator of structural stability between the protein and its ligands [58]. Unbound PBP2a (321.24) served as the baseline (Figure 9; Table 4). PBP2a complexed with  $\beta$ -sitosterol (325.43), ergosta-4,6,8 (322.17) and ergosterol (322.30) showed slightly increased stability, suggesting that these complexes had a slightly higher number of hydrogen bonds compared to unbound PBP2a, signifying potential stabilization effects due to ligand binding. PBP2a complexed with amoxicillin (321.44), 4-azaphenanthrene (321.15) and dehydroergosterol (320.83) had relative similar number of hydrogen bonds as the apo-PBP2a, indicating that the ligands did not significantly alter the number of hydrogen bonds in PBP2a following binding. PBP2a complexed with triphenyl phosphate (318.97) showed slightly decreased stability, as the complex had a slightly lower number of hydrogen bonds.

## 3.10 | Bond Analysis of Top-Ranked Compounds Against PBP2a at Different Timeframes During the 100 ns MD Simulation Period

Several thermodynamic factors, including the flexibility of amino acid residues, protein stability and compactness, and—above all—the number and nature of interactions with a protein's essential amino acids, influence a ligand's capacity to bind and inactivate a protein [58, 59]. Thus, in the present study, both the



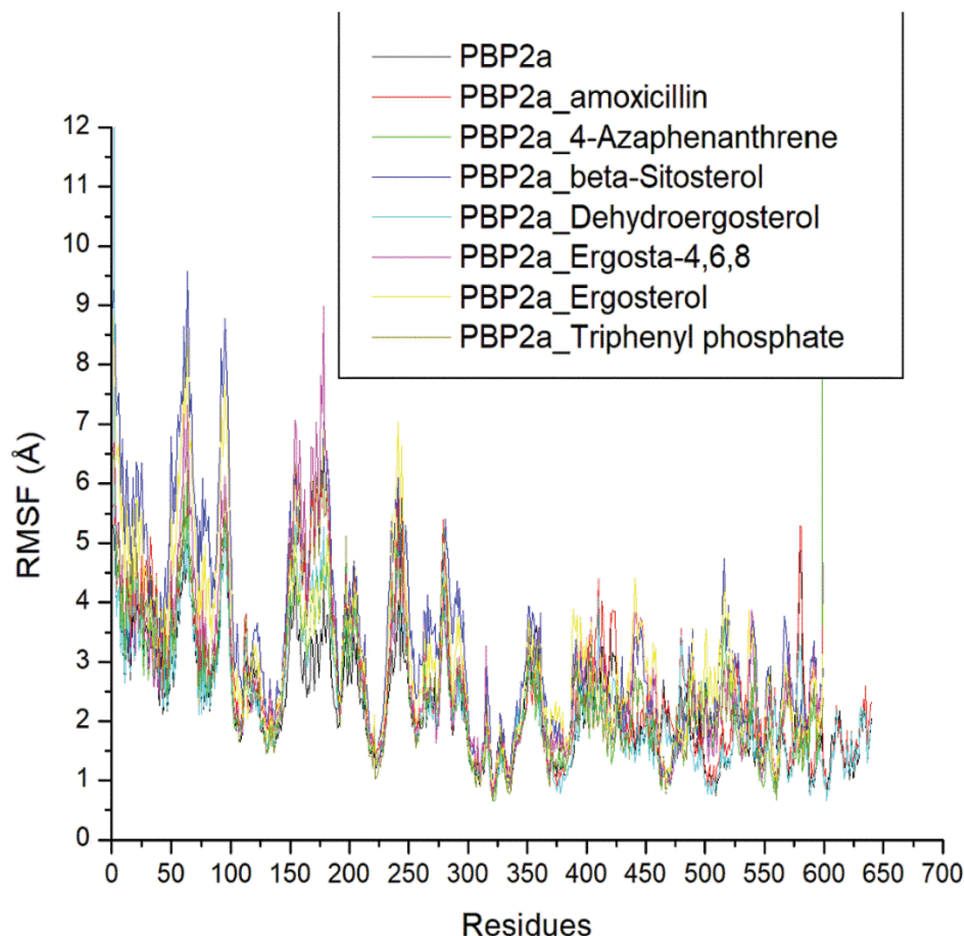


**FIGURE 7** | Comparative root means square fluctuation (RMSF) plots of alpha-carbon, the top six compounds, and standard, amoxicillin against residues of penicillin-binding protein 2a (PBP2a) after 100 ns molecular dynamic (MD) simulation. The active site residues noted in Figure 1 were observed to be outside the region of higher residue fluctuations found before the 250 amino acid residues.

number and nature of binding interactions that the top-ranked compounds established with PBP2a at various time intervals were examined (Table 5 and Table S7). Among the top-ranked compounds, dehydroergosterol and  $\beta$ -sitosterol with the highest binding free energy against PBP2a had the highest number of total interactions at 0, 50 and 100 ns timeframe (Table 5 and Table S7). This observation, while pointing to the correlation of total interactions with higher binding free energy of the top-ranked with PBP2a, is in tandem with prior studies on the importance of total interactions on higher negative binding free energy [55, 58]. However, the consistent and higher number of hydrogen bond interactions in dehydroergosterol complex with PBP2a relative to  $\beta$ -sitosterol-PBP2a with comparable the same number of interactions might have influenced to have higher binding free energy. Hydrogen-bond interactions are an important non-covalent bond in drug discovery, as they exhibit unusually strong intermolecular interactions. Hence, their consistency during a simulation could contribute immensely to higher binding free energy [60]. The importance of total interactions on higher binding free energy was also evident in PBP2a-4-azaphenanthrene complex with the lowest negative binding free energy correlating with its least number of interactions at each of the timeframe investigated. Importantly, the sharp decline in total number of interactions from 12 at 50 ns to 0 at 100 ns in PBP2a\_4-azaphenanthrene complex might have negatively influenced the ability of 4-

azaphenanthrene modulating PBP2a when compared to other top-ranked compounds. The observation on the modulation of PBP2a by amoxicillin is facilitated majorly by hydrogen bond which decreases as the MD simulation progress, whereas that of the top-ranked compounds with PBP2a is aided primarily by other important non-covalent bonds such as alky and pi-alky (Table S7). Generally, except for amoxicillin at 0 ns, none of the investigated compounds interacted with the catalytic residue Ser403 present in PBP2a active site [61], suggesting the partial occupancy of the top-ranked and amoxicillin during the MD simulation.

The most promising compounds from *G. lasiocarpa* endophytic fungi that could be developed as lead antibacterial agents against MRSA include 4-azaphenanthrene, 1,2-dimethyl-4-phenylethynyl from *A. fumigatus* (MK243451.1); triphenyl phosphate from *M. guilliermondii*; and ergosta-4,6,8(14),22-tetraen-3-one, ergosterol,  $\beta$ -sitosterol and dehydroergosterol 3,5-dinitrobenzoate from *P. raistrickii*.  $\beta$ -Sitosterol, one of the active substances isolated from the methanol extract of *Anadenanthera colubrina* fruits, demonstrated antifungal activity against *A. alternata* [62].  $\beta$ -Sitosterol, isolated from *A. alternata*, an endophytic fungus associated with *Morus alba* Linn., possesses antidiabetic properties [63]. It has also been reported to have anticancer, anti-inflammatory, antioxidant, cardioprotective, hepatoprotective and anti-allergic activities [64].



TABLE 5 | (Continued)

S/N	PBP2a complexes	Time (ns)		
		0	50	100
3.	PBP2a_beta-Sitosterol			
4.	PBP2a_Dehydroergosterol			
5.	PBP2a_Ergosta-4,6,8			

(Continues)

TABLE 5 | (Continued)

S/N	PBP2a complexes	Time (ns)		
		0	50	100
6.	PBP2a_Ergosterol	<p>Interactions</p> <ul style="list-style-type: none"> <li>van der Waals</li> <li>Pi-Alkyl</li> <li>Conventional Hydrogen Bond</li> </ul>	<p>Interactions</p> <ul style="list-style-type: none"> <li>van der Waals</li> <li>Pi-Alkyl</li> <li>Conventional Hydrogen Bond</li> </ul>	<p>Interactions</p> <ul style="list-style-type: none"> <li>van der Waals</li> <li>Pi-Alkyl</li> <li>Conventional Hydrogen Bond</li> </ul>
7.	PBP2a_Triphenyl phosphate	<p>Interactions</p> <ul style="list-style-type: none"> <li>van der Waals</li> <li>Pi-Donor Hydrogen Bond</li> <li>Pi-Pi T-shaped</li> <li>Pi-Alkyl</li> </ul>	<p>Interactions</p> <ul style="list-style-type: none"> <li>van der Waals</li> <li>Pi-Pi T-shaped</li> <li>Pi-Alkyl</li> </ul>	<p>Interactions</p> <ul style="list-style-type: none"> <li>van der Waals</li> <li>Pi-Alkyl</li> <li>Conventional Hydrogen Bond</li> </ul>



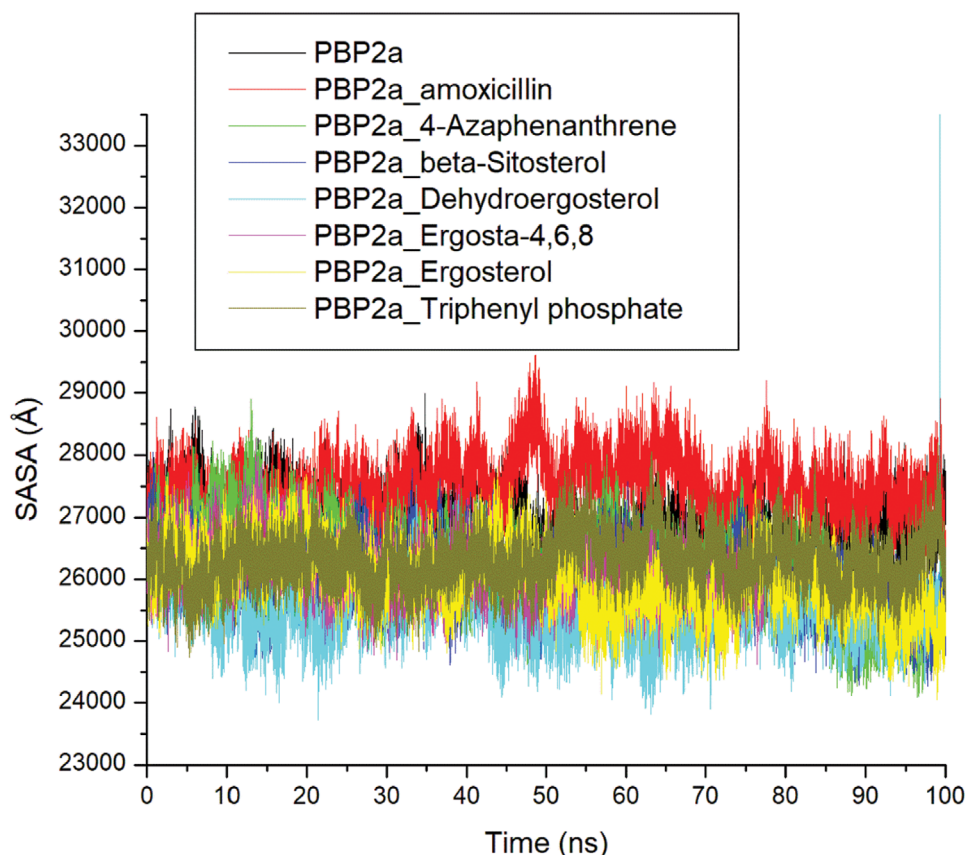


**FIGURE 8** | Comparative solvent-accessible surface area (SASA) plots of alpha-carbon, top six compounds and standard (amoxicillin) against the active site of penicillin-binding protein 2a (PBP2a) of *Staphylococcus aureus* over 100 ns molecular dynamic (MD) simulation period. The figure reflects the overall compactness and folding of the PBP2a complexed with the top six compounds compared to that of the reference standard and the alpha-carbon of PBP2a. Relative to the reference standard and the alpha-carbon of PBP2a, all the complexes formed against PBP2a by the top six compounds were observed to be compact.

Ergosterol was identified in the extract of *A. alternata* HE11, obtained from *Colocasia esculenta* leaves. This compound exhibited antibacterial activity against *S. aureus* ATCC 25923 and *Staphylococcus faecalis* ATCC 8043 [65]. Ergosta-4,6,8(14),22-tetraen-3-one, derived from *Pholiota adiposa*, possesses antidiabetic properties [66] and has also been isolated from *Ganoderma tuberculosum* (Agaricomycetes), where it exhibits antiparasitic properties [67]. The reported antibacterial activities of ergosterol,  $\beta$ -sitosterol and dehydroergosterol 3,5-dinitrobenzoate may explain the inhibitory activities against MRSA and *S. aureus* observed in the range of 62.5–1000  $\mu$ g/mL.

### 3.11 | Pharmacokinetics and Physicochemical Properties of the Top Six Metabolites of *G. lasiocarpa* Extract

The physicochemical properties of the top six metabolites of *G. lasiocarpa* extract are presented in Table 6. According to Lipinski's rule of five, compounds are likely to be well-absorbed and highly permeable if they meet the following criteria: a molecular weight under 500 g/mol, a partition coefficient (log P) below 5, fewer than 10 hydrogen bond acceptors and fewer than 5 hydrogen bond donors [68]. Except for dehydroergosterol, the top-ranked compounds fulfilled the Lipinski's rule of five suggestive of their potential to be orally bioavailable to reach druggable

targets in cells. Similarly, except for dehydroergosterol, the top-ranked compounds are non-inhibitors of CYP3A4 responsible for metabolizing up to 50% of all clinically used drug [69], suggesting that the top-ranked metabolites will rarely result in drug-drug interactions when used with other drugs being metabolised by CYP3A4. Although ergosterol, triphenyl phosphate, and  $\beta$ -sitosterol have a lower lethal dose 50 (LD<sub>50</sub>) that classified them as molecules that might be toxic, dehydroergosterol, ergosta-4,6,8 and 4-azaphenanthrene had LD<sub>50</sub> that classified them as drug classes four, five and six that are suitable for drug development. Considering the better binding free energy of dehydroergosterol in this study relative to other compounds, the prediction that the compound might lack oral bioavailability might mean that further structural optimization of the compound might be needed, especially as the compound also had poor solubility relative to amoxicillin that is soluble. Studies have correlated poor solubility to pharmacologic potency and permeability [70].

## 4 | Conclusions

A rich diversity of endophytic fungi species is nested in the leaves and stem bark of *G. lasiocarpa* and their extract contains several phytochemicals. The five isolated and identified endophytic fungi, *P. raistrickii* (MK243492.1), *P. spinulosum* (MK243479.1), *M. guilliermondii* (MK243634.1), *A. fumigatus* (MK243451.1) and

TABLE 6 | Pharmacokinetics and physicochemical properties of amoxicillin (reference compound) and the top six metabolites of *Grewia lasiocarpa* E. Mey. Ex Harv. extract.

Ligands zinc code	MW < 500 (g/mol)	HB-A ≤10	HB-D ≤5	Log Po/w ≤5	RT-B ≤9	WS	GI-A	BS	Pgp	Inhibitor of CYP 450s								C	IM	M	CY	TC	LD <sub>50</sub> (mg/kg)
										CYP 1A2	CYP 2C19	CYP 2C9	CYP 2D6	CYP 3A4	H								
Amoxicillin	365.4	6	4	−0.39	5	VS	L	0.55	N	N	N	N	N	N	I	I	I	I	I	6	15000		
4-Azaphenanthrene	210.31	0	0	4.78	2	PS	L	0.55	N	N	N	N	Y	N	I	A	I	I	I	5	2333		
β-Sitosterol	414.71	1	1	7.19	6	PS	L	0.55	N	N	N	N	N	N	I	I	A	I	I	4	890		
Dehydroergosterol	588.73	6	0	6.25	9	PS	L	0.17	Y	N	N	Y	N	Y	I	I	A	I	I	4	2000		
Ergosta-4,6,8	392.62	1	0	6.35	4	MS	L	0.55	N	N	N	Y	N	N	I	I	I	I	I	6	10000		
Ergosterol	396.65	1	1	6.49	4	MS	L	0.55	N	N	N	Y	N	N	I	I	A	I	I	2	10		
Triphenyl phosphate	326.28	4	0	4.06	6	PS	H	0.55	N	Y	Y	Y	Y	N	I	I	I	I	I	4	1320		

Note: MW, Molecular weight; HB-A, Hydrogen bond acceptor; HB-D, Hydrogen bond donor; Log Po/w, Partition coefficient; RT-B, rotatable bond; WS, Water solubility; GI- A, Gastrointestinal absorption; Pgp, Permeability glycoprotein substrate; CYP, Cytochrome; VS, very soluble; MS, Moderately soluble; S, Soluble; PS, poorly soluble, N, No; Y, Yes; L, low; I, Inactive; A, Active; BS, Bioavailability score; H, Hepatotoxicity; C, Carcinogenicity; IM, Immunotoxicity; M, Mutagenicity; CY, Cytotoxicity; LD, Lethal dose; TC, Toxicity class; SA, Synthetic accessibility; and BA, binding affinity.

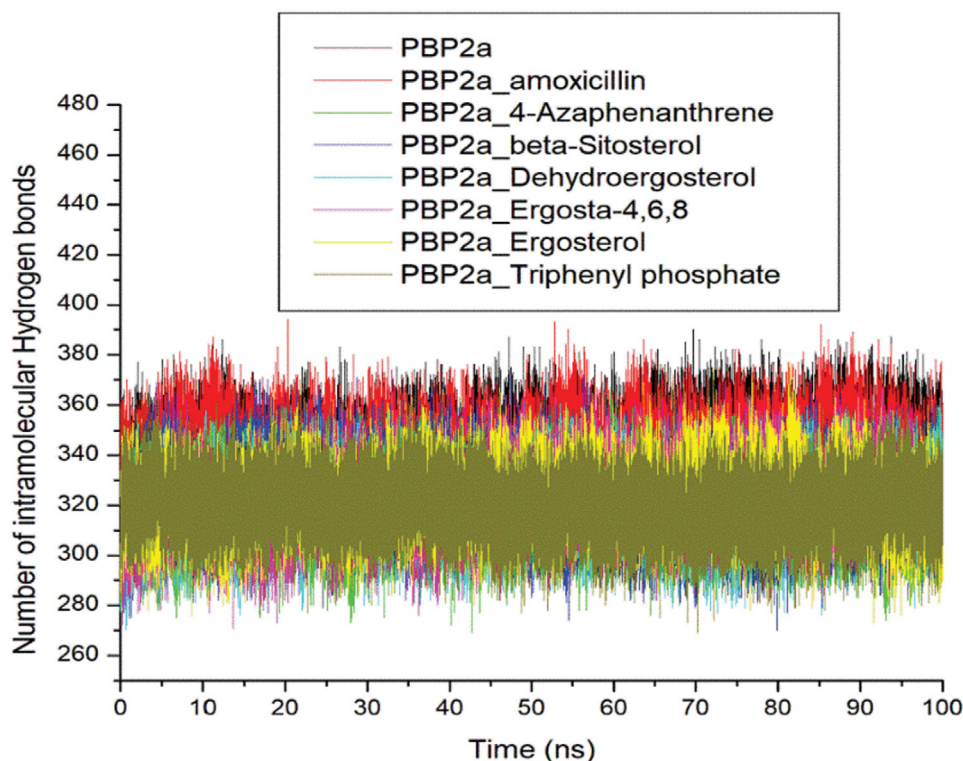


**FIGURE 9** | Time evolution of the number of intramolecular hydrogen bonds and distance in penicillin-binding protein 2a (PBP2a) following the binding of the standard amoxicillin and the top six compounds at the active site of PBP2a of *Staphylococcus aureus* during the 100 ns molecular dynamic (MD) simulation period.

*A. fumigatus* (MK243397.1) are promising sources of antibacterial compounds against MRSA and antioxidants. In silico exploration of the metabolites of the extract against PBP2a (implicated majorly in the broad clinical resistance of MRSA to most conventional beta-lactams) identified the potential of the phytosterol constituent (dehydroergosterol, ergosterol and  $\beta$ -sitosterol) of the extract as potential modulators of PBP2a. The phytosterol constituent and most especially dehydroergosterol had good stability, compactness and interactions with PBP2a during the 100 ns MD simulation, reinforcing their potential as compounds that may be developed as beta-lactam against infections caused by MRSA. Hence, the endophytic extracts from the leaves and stem bark of *G. lasiocarpa* harbour pharmacologically active secondary metabolites and most especially the phytosterol constituent. However, the prediction that the lead compound (dehydroergosterol) from the extracts lacks oral bioavailability with poor water solubility means that further structural optimization of dehydroergosterol might be needed for druggability improvement. To this best of our knowledge, this is the first report on the isolation, identification, characterization, in vitro and in silico antibacterial exploration of fungal endophytes from the leaves and stem bark of *G. lasiocarpa*. Future study will focus on isolating dehydroergosterol in the five endophytic fungi and exploring its anti-PBP2a modulatory role in vitro and in vivo.

## Accession Numbers

The comparison of the Internal Transcribed Spacer (ITS) sequences from GLANA1, GLANA2, GLANA3, GLANA4 and

GLANA5 when compared with GenBank database revealed that the five endophytic fungi are GLANA1: *Aspergillus fumigatus* (accession number MK243397.1), GLANA2: *Aspergillus fumigatus* (accession number MK243451.1), GLANA3: *Penicillium spinulosum* (accession number MK243479.1), GLANA4: *Penicillium raistrickii* (accession number MK243492.1) and GLANA5: *Meyerozyma guilliermondii* (accession number MK243634.1).

## Author Contributions

**Nneka Augustina Akwu:** designed the study, implemented and prepared the draft manuscript, isolated and characterised the endophytic fungi and conducted the phytochemical, antimicrobial and antioxidant assay. **Jamiu Olaseni Aribisala** and **Saheed Sabiu** conducted the *in silico* analyses. **Yogasphree Naidoo, Moganavelli Singh, Johnson Lin, Jamiu Olaseni Aribisala, Saheed Sabiu, Makhotso Lekhooa and Adeyemi Oladapo Aremu:** supervised the study and revised the manuscript.

## Acknowledgments

N.A.A. would like to gratefully acknowledge the Organization for Women in Science for the Developing World (OWSD) and Swedish International Development Cooperation Agency for their financial support. We appreciate the National Research Foundation for financial support used in the purchase of the consumables used for this study. We are also grateful to Dr. Chunderika Mocktar for the provision of the clinical bacteria strains.

## Conflicts of Interest

The authors declare no conflicts of interest.

## Data Availability Statement

The data that support the findings of this study are available as part of the Supporting Information of this article.

## References

1. a) M. W. Iwu, A. R. Duncan, and C. O. Okunji, "New Antimicrobials of Plant Origin," in *Perspectives on New Crops and New Uses*, ed. J. Janick (Alexandria, VA: ASHS Press, 1999), 457–462. b) B. Baral, K. Mamale, S. Gairola, C. Chauhan, A. Dey, and R. K. Kaundal, "Infectious Diseases and Its Global Epidemiology," in *Nanostructured Drug Delivery Systems in Infectious Disease Treatment*, eds. S. Beg, R. Shukla, M. Handa, M. Rahman, and A. Dhira (Amsterdam: Academic Press, 2024), 1–24, <https://doi.org/10.1016/B978-0-443-13337-4.00017-3>.
2. a) R. Wise, "The Worldwide Threat of Antimicrobial Resistance," *Current Science* 95 (2008): 181–187. Accessed December 28, 2024, <http://www.jstor.org/stable/2410304>. b) E. M. Abdallah, B. Y. Alhatlani, R. de Paula Menezes, and C. H. G. Martins, "Back to Nature: Medicinal Plants as Promising Sources for Antibacterial Drugs in the Post-Antibiotic Era," *Plants* 12 (2023): 3077. c) O. Ožegić, B. Bedenić, S. L. Sternak, et al., "Antimicrobial Resistance and Sports: The Scope of the Problem, Implications for Athletes' Health and Avenues for Collaborative Public Health Action," *Antibiotics* 13 (2024): 232.
3. A. Alvin, K. I. Miller, and B. A. Neilan, "Exploring the Potential of Endophytes From Medicinal Plants as Sources of Antimicrobial Compounds," *Microbiological Research* 169 (2014): 483–495.
4. a) V. Mathur and D. Ulanova, "Microbial Metabolites Beneficial to Plant Hosts Across Ecosystems," *Microbial Ecology* 86 (2023): 25–48. b) M. S. M. Selim, S. A. Abdelhamid, and S. S. Mohamed, "Secondary Metabolites and Biodiversity of Actinomycetes," *Journal of Genetic Engineering and Biotechnology* 19 (2021): 72.
5. S. Mishra, A. Bhattacharjee, and S. Sharma, "An Ecological Insight into the Multifaceted World of Plant–Endophyte Association," *Critical Reviews in Plant Sciences* 40 (2021): 127–146.
6. V. K. Singh and A. Kumar, "Secondary Metabolites From Endophytic Fungi: Production, Methods of Analysis, and Diverse Pharmaceutical Potential," *Symbiosis* 90 (2023): 111–125.
7. A. H. Hashem, M. S. Attia, E. K. Kandil, et al., "Bioactive Compounds and Biomedical Applications of Endophytic Fungi: A Recent Review," *Microbial Cell Factories* 22 (2023): 107.
8. a) H. Lu, T. Wei, H. Lou, X. Shu, and Q. Chen, "A Critical Review on Communication Mechanism Within Plant–Endophytic Fungi Interactions to Cope with Biotic and Abiotic Stresses," *Journal of Fungi* 7 (2021): 719. b) A. Verma, N. Shameem, H. S. Jatav, et al., "Fungal Endophytes to Combat Biotic and Abiotic Stresses for Climate-Smart and Sustainable Agriculture," *Frontiers in Plant Science* 13 (2022): 953836.
9. a) J. S. Kushveer, M. Rashmi, and V. V. Sarma, "Bioactive Compounds From Marine-Derived Fungi and Their Potential Applications," in *Fungi Bio-Prospects in Sustainable Agriculture, Environment and Nano-Technology*, eds. V. K. Sharma, M. P. Shah, S. Parmar, and A. Kumar (Amsterdam: Academic Press, 2021), 91–173, <https://doi.org/10.1016/B978-0-12-821734-4.00014-9>. b) P. Tiwari and H. Bae, "Endophytic Fungi: Key Insights, Emerging Prospects, and Challenges in Natural Product Drug Discovery," *Microorganisms* 10 (2022): 360.
10. R. Boon and E. Pooley, *Pooley's Trees of Eastern South Africa* (Durban, KwaZulu-Natal, SA: Flora and Fauna Publications Trust, 2010).
11. a) S. K. Deshmukh and R. N. Kharwar, "Fungi a Potential Source of Bioactive Metabolites an Indian Prospective," in *Progress in Mycology: Biology and Biotechnological Applications*, eds. T. Satyanarayana, S. K. Deshmukh, and M. V. Deshpande (Singapore: Springer Nature Singapore, 2022), 461–516, [10.1007/978-981-16-3307-2\\_16](https://doi.org/10.1007/978-981-16-3307-2_16). b) R. Deshidi, S. Devari, M. Kushwaha, et al., "Isolation and Quantification of Alternariols From Endophytic Fungus, *Alternaria alternata*: LC–ESI–MS/MS Analysis," *ChemistrySelect* 2 (2017): 364–368. c) A. Magotra, M. Kumar, M. Kushwaha, et al., "Epigenetic Modifier Induced Enhancement of fumiquinazoline C production in *Aspergillus fumigatus* (GA-L7): An Endophytic Fungus From *Grewia asiatica* L.," *Applied Microbiology and Biotechnology Express* 7 (2017): 43.
12. W. Beinart and K. Brown, *African Local Knowledge & Livestock Health: Diseases & Treatments in South Africa*, NED-New edn. (Suffolk: Boydell & Brewer Ltd, 2013), <http://www.jstor.org/stable/10.7722/j.ctt3fgmqw>.
13. a) N. Akwu, Y. Naidoo, M. Singh, N. Nundkumar, and J. Lin, "Phytochemical Screening, In Vitro Evaluation of the Antimicrobial, Antioxidant and Cytotoxicity Potentials of *Grewia lasiocarpa* E. Mey. ex Harv.," *South African Journal of Botany* 123 (2019): 180–192. b) N. A. Akwu, Y. Naidoo, S. T. Channangihalli, M. Singh, N. Nundkumar, and J. Lin, "The Essential Oils of *Grewia lasiocarpa* E. Mey. Ex Harv.: Chemical Composition, In Vitro Biological Activity and Cytotoxic Effect on Hela Cells," *Anais da Academia Brasileira de Ciências* 93 (2021): e20190343.
14. M. Rahman, K. Amin, S. Rahman, et al., "Investigation of Methicillin-Resistant *Staphylococcus aureus* Among Clinical Isolates From Humans and Animals by Culture Methods and Multiplex PCR," *BMC Veterinary Research* 14 (2018): 300.
15. A. E. Davies, R. L. Williams, G. Lugano, S. R. Pop, and V. R. Kearns, "In Vitro and Computational Modelling of Drug Delivery Across the Outer Blood–Retinal Barrier," *Interface Focus* 10 (2020): 20190132.
16. G. Strobel and B. Daisy, "Bioprospecting for Microbial Endophytes and their Natural Products," *Microbiology and Molecular Biology Reviews* 67 (2003): 491–502.
17. M. Luginbühl, "Endophytische Pilze bei Buxus, Hedera, Ilex und Ruscus," (PhD diss., ETH Zürich, Switzerland, 1980).
18. C. W. Bacon and J. F. White, "Stains, Media, and Procedures for Analyzing Endophytes," *Biotechnology of Endophytic Fungi of Grasses*, 1st edn, ed. C. W. Bacon (Boca Raton, FL: CRC Press, 2018).
19. A. M. Pirttilä and S. Sorvari, eds., *Prospects and Applications for Plant-Associated Microbes – A Laboratory Manual: Part B: Fungi* (Finland: BioBion Innovations, 2014).
20. H. W. Zhang, Y. C. Song, and R. X. Tan, "Biology and Chemistry of Endophytes," *Natural Product Reports* 23 (2006): 753–771.
21. a) M. Talontsi, *Novel Antimycotic Epicoccoides, Sordariones and Further New Zoosporicidal Natural Products From Endophytic Fungi Inhabiting Cameroonian Medicinal Plants* (Sweden: Brimstone Publisher, 2011). b) M. Rosenblueth and E. Martinez-Romero, "Bacterial Endophytes and Their Interactions With Hosts," *Molecular Plant-Microbe Interactions* 19 (2006): 827–837.
22. a) J. Coates, "Interpretation of Infrared Spectra, A Practical Approach," in *Encyclopedia of Analytical Chemistry*, eds. R. A. Meyers and M. L. McKelvy (Chichester: John Wiley & Sons Ltd, 2006), 10815–10837, <https://doi.org/10.1002/9780470027318.a5606>. b) B. Stuart, "Infrared Spectroscopy," in *Analytical Techniques in Forensic Science* edited by R. Wolstenholme, S. Jickells, S. Forbes (West Sussex, UK: John Wiley & Sons Ltd, 2021), 145–160, <https://onlinelibrary.wiley.com/doi/book/10.1002/9781119373421>.
23. C. Perez, "Antibiotic Assay by Agar-Well Diffusion Method," *Acta Biologica Et Medicinae Experimentalis* 15 (1990): 113–115.
24. A. Braca, C. Sortino, M. Politi, I. Morelli, and J. Mendez, "Antioxidant Activity of Flavonoids From *Licania licaniaeflora*," *Journal of Ethnopharmacology* 79 (2002): 379–381.
25. O. Oyebode, O. L. Erukainure, L. Zuma, C. U. Ibeji, N. A. Koobanally, and M. S. Islam, "In Vitro and Computational Studies of the Antioxidant and Anti-Diabetic Properties of *Bridelia ferruginea*," *Journal of Biomolecular Structure and Dynamics* 40 (2022): 3989–4003.
26. S. F. Altschul, T. L. Madden, A. A. Schäffer, et al., "Gapped BLAST and PSI-BLAST: A New Generation of Protein Database Search Programs," *Nucleic Acids Research* 25 (1997): 3389–3402.
27. S. Kumar, G. Stecher, and K. Tamura, "MEGA7: Molecular Evolutionary Genetics Analysis Version 7.0 for Bigger Datasets," *Molecular Biology and Evolution* 33 (2016): 1870–1874.



28. L. H. Otero, A. Rojas-Altuve, L. I. Llarrull, et al., "How Allosteric Control of *Staphylococcus aureus* Penicillin Binding Protein 2a Enables Methicillin Resistance and Physiological Function," *Proceedings of the National Academy of Sciences* 110 (2013): 16808–16813.
29. F. M. Al-Khodairy, M. K. A. Khan, M. Kunhi, M. S. Pulicat, S. Akhtar, and J. M. Arif, "In Silico Prediction of Mechanism of Erythrin-Induced Apoptosis in Human Breast Cancer Cell Lines," *American Journal of Bioinformatics Research* no. 3 (2013): 62–71.
30. S. Sabiu, F. O. Balogun, and S. O. Amoo, "Phenolics Profiling of *Carpobrotus edulis* (L.) N.E.Br. and Insights Into Molecular Dynamics of Their Significance in Type 2 Diabetes Therapy and Its Retinopathy Complication," *Molecules (Basel, Switzerland)* 26 (2021): 4867.
31. a) R. Oktiansyah, E. Elfita, H. Widjajanti, A. Setiawan, M. Mardiyanto, and S. S. Nasution, "Antioxidant and Antibacterial Activity of Endophytic Fungi Isolated From the Leaves of Sungkai (*Peronema canescens*)," *Tropical Journal of Natural Product Research* 7, no. 3 (2023): 2596–2604. b) I. M. Ababutain, S. K. Aldosary, A. A. Aljuraifani, et al., "Identification and Antibacterial Characterization of Endophytic Fungi From *Artemisia sieberi*," *International Journal of Microbiology* 2021 (2021): 6651020.
32. N. Akwu, Y. Naidoo, M. Singh, S. C. Thimmegowda, N. Nundkumar, and J. Lin, "Isolation of Lupeol From *Grewia lasiocarpa* Stem Bark: Antibacterial, Antioxidant, and Cytotoxicity Activities," *Biodiversitas Journal of Biological Diversity* 21 (2020): 5684–5690.
33. N. K. Afseth and A. Kohler, "Extended Multiplicative Signal Correction in Vibrational Spectroscopy, a Tutorial," *Chemometrics and Intelligent Laboratory Systems* 117 (2012): 92–99.
34. a) S. I. Khalivulla, A. Mohammed, K. N. Sirajudeen, M. I. Shaik, W. Ye, and M. Korivi, "Novel Phytochemical Constituents and Anticancer Activities of the Genus, *Typhonium*," *Current Drug Metabolism* 20 (2019): 946–957. b) Y. Nalli, D. N. Mirza, Z. A. Wani, et al., "Phialomustin A–D, New Antimicrobial and Cytotoxic Metabolites From an Endophytic Fungus, *Phialophora mustea*," *Royal Society of Chemistry Advances* 5 (2015): 95307–95312.
35. M. Abdul Qadir, S. K. Shahzadi, A. Bashir, A. Munir, and S. Shahzad, "Evaluation of Phenolic Compounds and Antioxidant and Antimicrobial Activities of Some Common Herbs," *International Journal of Analytical Chemistry* 2017 (2017): 3475738.
36. a) Y. Yang and T. Zhang, "Antimicrobial Activities of Tea Polyphenol on Phytopathogens: A Review," *Molecules (Basel, Switzerland)* 24 (2019): 816. b) K. Ecevit, A. A. Barros, J. M. Silva, and R. L. Reis, "Preventing Microbial Infections With Natural Phenolic Compounds," *Future Pharmacology* 2 (2022): 460–498.
37. a) I. H. Khan and A. Javaid, "In Vitro Screening of *Aspergillus* spp. for Their Biocontrol Potential Against *Macrophomina phaseolina*," *Journal of Plant Pathology* 103 (2021): 1195–1205. b) N. Venkateswarulu, S. Shameer, P. Bramhachari, S. T. Basha, C. Nagaraju, and T. Vijaya, "Isolation and Characterization of Plumbagin (5-Hydroxy-2-Methylnaptalene-1,4-Dione) Producing Endophytic Fungi *Cladosporium delicatulum* From Endemic Medicinal Plants," *Biotechnology Reports* 20 (2018): e00282.
38. K. Jawaid, M. Shafique, A. Versiani, H. Muhammed, S. A. Naz, and N. Jabeen, "Antimicrobial Potential of Newly Isolated *Aspergillus terreus* MK-1: An Approach Towards New Antibiotics," *The Journal of the Pakistan Medical Association* 69 (2019): 18–23.
39. S. Kumar, R. Saini, P. Suthar, V. Kumar, and R. Sharma, *Plant Secondary Metabolites: Physico-Chemical Properties and Therapeutic Applications* (Berlin: Springer, 2022).
40. J. Liu, C. Du, H. T. Beaman, and M. B. B. Monroe, "Characterization of Phenolic Acid Antimicrobial and Antioxidant Structure–Property Relationships," *Pharmaceutics* 12 (2020): 419.
41. E. H. Stukenbrock, "Speciation Genomics of Fungal Plant Pathogens," in *Advances in Botanical Research*, vol. 70, ed. F. M. Martin (Amsterdam: Academic Press, 2014), 397–423.
42. a) Y.-J. Chen, Y.-Q. Sun, R.-Q. Zhang, et al., "A New Phenolic Compound From Endophytic Fungus *Aspergillus fumigatus* of *Euphorbia royleana*," *China Journal of Chinese Materia Medica* 44 (2019): 5429–5432. b) S. S. El-Hawary, A. S. Moawad, H. S. Bahr, U. R. Abdelmohsen, and R. Mohammed, "Natural Product Diversity From the Endophytic Fungi of the Genus *Aspergillus*," *Royal Society of Chemistry Advances* 10 (2020): 22058–22079.
43. H. Jin, Z. Yan, Q. Liu, X. Yang, J. Chen, and B. Qin, "Diversity and Dynamics of Fungal Endophytes in Leaves, Stems and Roots of *Stellera chamaejasme* L. in Northwestern China," *Antonie Van Leeuwenhoek* 104 (2013): 949–963.
44. C. Lee and S. H. Shim, "Endophytic Fungi Inhabiting Medicinal Plants and their Bioactive Secondary Metabolites," *Natural Product Sciences* 26 (2020): 10–27.
45. M. Ravuri and S. Shivakumar, "Optimization of Conditions for Production of Lovastatin, a Cholesterol Lowering Agent, from a Novel Endophytic Producer *Meyerozyma guilliermondii*," *Journal of Biologically Active Products From Nature* 10 (2020): 192–203.
46. A. G. Ogofure, S. P. Pelo, and E. Green, "Identification and Assessment of Secondary Metabolites from Three Fungal Endophytes of *Solanum mauritanum* against Public Health Pathogens," *Molecules (Basel, Switzerland)* 29 (2024): 4924.
47. E. İzol and M. Turhan, "In-Depth Phytochemical Profile by LC–MS/MS, Mineral Content by ICP–MS, and In-Vitro Antioxidant, Antidiabetic, Antiepilepsy, Anticholinergic, and Antiglaucoma Properties of Bitlis Propolis," *Life* 14 (2024): 1389.
48. M.-D. Wu, M.-J. Cheng, W.-Y. Wang, et al., "Antioxidant Activities of Extracts and Metabolites Isolated from the Fungus *Antrodia cinnamomea*," *Natural Product Research* 25 (2011): 1488–1496.
49. N. Abdel-Monem, A. M. Abdel-Azeem, E. El Ashry, D. A. Ghareeb, and A. Nabil-Adam, "Assessment of Secondary Metabolites from Marine-Derived Fungi as Antioxidant," *Open Journal of Medicinal Chemistry* 3 (2013): 60–73.
50. M. A. Karaman, N. M. Mimica-Dukić, and M. N. Matavulj, "Lignicolous Fungi as Potential Natural Sources of Antioxidants," *Archives of Biological Sciences* 57 (2005): 93–100.
51. D. R. Alves, W. M. B. da Silva, D. L. dos Santos, F. d. C. de Oliveira Freire, F. R. Vasconcelos, and S. M. de Moraes, "Atividades Antioxidante, Anticolinesterásica e Citotóxica de Metabolitos de Fungos Endofíticos/Antioxidant, Anticolinesterasic and Cytotoxic Activities of Endophytic Fungus Metabolites," *Brazilian Journal of Development* 6 (2020): 73684–73691.
52. a) E. Perola, W. P. Walters, and P. S. Charifson, "A Detailed Comparison of Current Docking and Scoring Methods on Systems of Pharmaceutical Relevance," *Proteins: Structure, Function, and Bioinformatics* 56 (2004): 235–249. b) K. Onodera, K. Satou, and H. Hirota, "Evaluations of Molecular Docking Programs for Virtual Screening," *Journal of Chemical Information and Modeling* 47 (2007): 1609–1618. c) D. Plewczynski, M. Łażniewski, R. Augustyniak, and K. Ginalski, "Can We Trust Docking Results? Evaluation of Seven Commonly Used Programs on PDBbind Database," *Journal of Computational Chemistry* 32 (2011): 742–755.
53. a) A. Zapun, C. Contreras-Martel, and T. Vernet, "Penicillin-Binding Proteins and  $\beta$ -Lactam Resistance," *FEMS Microbiology Reviews* 32 (2008): 361–385. b) E. Sauvage, F. Kerff, M. Terrak, J. A. Ayala, and P. Charlier, "The Penicillin-Binding Proteins: Structure and Role in Peptidoglycan Biosynthesis," *FEMS Microbiology Reviews* 32 (2008): 234–258.
54. H. Hata, D. P. Tran, M. M. Sobeh, and A. Kitao, "Binding Free Energy of Protein/Ligand Complexes Calculated Using Dissociation Parallel Cascade Selection Molecular Dynamics and Markov State model," *Biophysics and Microbiology* 18 (2021): 305–316.
55. J. O. Aribisala, R. A. Abdulsalam, Y. Dweba, K. Madonsela, and S. Sabiu, "Identification of Secondary Metabolites from *Crescentia cujete* as Promising Antibacterial Therapeutics Targeting Type 2A Topoisomerases Through Molecular Dynamics Simulation," *Computers in Biology and Medicine* 145 (2022): 105432.

56. J. O.-O. Uhomoibhi, F. O. Shode, K. A. Idowu, and S. Sabiu, "Molecular Modelling Identification of Phytocompounds from Selected African Botanicals as Promising Therapeutics against Druggable Human Host Cell Targets of SARS-CoV-2," *Journal of Molecular Graphics and Modelling* 114 (2022): 108185.
57. J. O. Aribisala, S. Nkosi, K. Idowu, et al., "Astaxanthin-Mediated Bacterial Lethality: Evidence from Oxidative Stress Contribution and Molecular Dynamics Simulation," *Oxidative Medicine and Cellular Longevity* 2021 (2021): 7159652.
58. X. Du, Y. Li, Y.-L. Xia, et al., "Insights into Protein-Ligand Interactions: Mechanisms, Models, and Methods," *International Journal of Molecular Sciences* 17 (2016): 144.
59. D. Ramirex and J. Caballero, "Is it Reliable to Use Common Molecular Docking Methods for Comparing the Binding Affinities of Enantiomer Pairs for their Protein Target?," *International Journal of Molecular Sciences* 17 (2016): 525–545.
60. H. Izadi, K. M. Stewart, and A. Penlidis, "Role of Contact Electrification and Electrostatic Interactions in Gecko Adhesion," *Journal of the Royal Society Interface* 11 (2014): 20140371.
61. D.-J. Scheffers and M. G. Pinho, "Bacterial Cell Wall Synthesis: New Insights From Localization Studies," *Microbiology and Molecular Biology Reviews* 69 (2005): 585–607.
62. V. A. Campos, F. J. Perina, E. Alves, J. Sartorelli, A. M. Moura, and D. F. Oliveira, "*Anadenanthera colubrina* (Vell.) Brenan Produces Steroidal Substances that are Active against *Alternaria alternata* (Fr.) Keissler and that may Bind to Oxysterol-Binding Proteins," *Pest Management Science* 70 (2014): 1815–1822.
63. a) S. Babu and S. Jayaraman, "An Update on  $\beta$ -Sitosterol: A Potential Herbal Nutraceutical for Diabetic Management," *Biomedicine & Pharmacotherapy* 131 (2020): 110702. b) V. Dwibedi, S. S. Mishra, N. George, et al., "Purification of Ursolic Acid and  $\beta$ -Sitosterol From Endophytic *Alternaria alternata* for Their Alpha-Amylase Inhibitory Activity," *Journal of Biomolecular Structure and Dynamics* 42, no. 13 (2024): 6688–6699.
64. a) Z. Khan, N. Nath, A. Rauf, et al., "Multifunctional Roles and Pharmacological Potential of  $\beta$ -Sitosterol: Emerging Evidence Toward Clinical Applications," *Chemico-Biological Interactions* 365 (2022): 110117. b) L. Ma, Y. Ma, and Y. Liu, " $\beta$ -Sitosterol Protects Against Food Allergic Response in BALB/c Mice by Regulating the Intestinal Barrier Function and Reconstructing the Gut Microbiota Structure," *Food and Function* 14 (2023): 4456–4469.
65. H. T. Khazaa, M. T. Khazaa, A. S. Abdel-Razek, et al., "Antimicrobial, Antiproliferative Activities and Molecular Docking of Metabolites From *Alternaria alternata*," *Applied Microbiology and Biotechnology Express* 13 (2023): 68.
66. X.-Y. Wang, S. Jiang, and Y. Liu, "Anti-Diabetic Effects of Fungal Ergosta-4, 6, 8(14), 22-Tetraen-3-One From *Pholiota adiposa*," *Steroids* 192 (2023): 109185.
67. V. Espinosa-García, J. J. Fernandez, D. San Nicolás-Hernández, et al., "Antiparasitic Activity of Compounds Isolated From *Ganoderma tuberculosum* (Agaricomycetes) from Mexico," *International Journal of Medicinal Mushrooms* 25 (2023): 63–72.
68. C. A. Lipinski, F. Lombardo, B. W. Dominy, and P. J. Feeney, "Experimental and Computational Approaches to Estimate Solubility and Permeability in Drug Discovery and Development Settings," *Advanced Drug Delivery Reviews* 23 (1997): 3–25.
69. I. F. Sevrioukova and T. L. Poulos, "Understanding the Mechanism of Cytochrome P450 3A4: Recent Advances and Remaining Problems," *Dalton Transactions* 42 (2013): 3116–3126.
70. D. V. Bhalani, B. Nutan, A. Kumar, and A. K. Singh Chandel, "Bioavailability Enhancement Techniques for Poorly Aqueous Soluble Drugs and Therapeutics," *Biomedicines* 10 (2022): 2055.

## Supporting Information

Additional supporting information can be found online in the Supporting Information section.